

Sterically Driven Metal-Free Oxidation of 2,7-Di-*tert*-butylpyrene

Tarek H. El-Assaad,¹ Keshaba N. Parida,¹ Marcello F. Cesario,¹ Dominic V. McGrath^{1,*}

¹ Department of Chemistry and Biochemistry, University of Arizona, Tucson, AZ 85721.

Supporting Information

Table of Contents

I.	General Summary	S2-S4
II.	General Remarks	S4
III.	Synthetic Procedures	S5-S16
IV.	Summary of Characterization Data	S17-S18
V.	Visual Aids	S19-S20
VI.	Green Chemistry Metrics	S21-S22
VII.	NMR Spectra	S23-S39
VIII.	UV-Vis, HRMS, IR Data	S40-S48
IX.	References	S49

* To whom correspondence should be addressed. Email: mcgrath@email.arizona.edu

I. General Summary:

Table S1. Reference chart for compounds in this work (red = not synthesized).

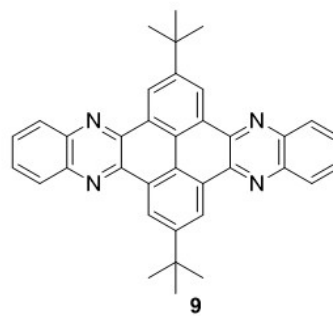
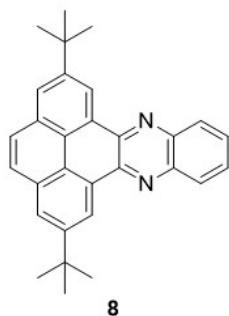
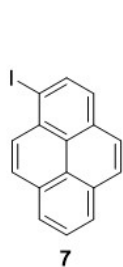
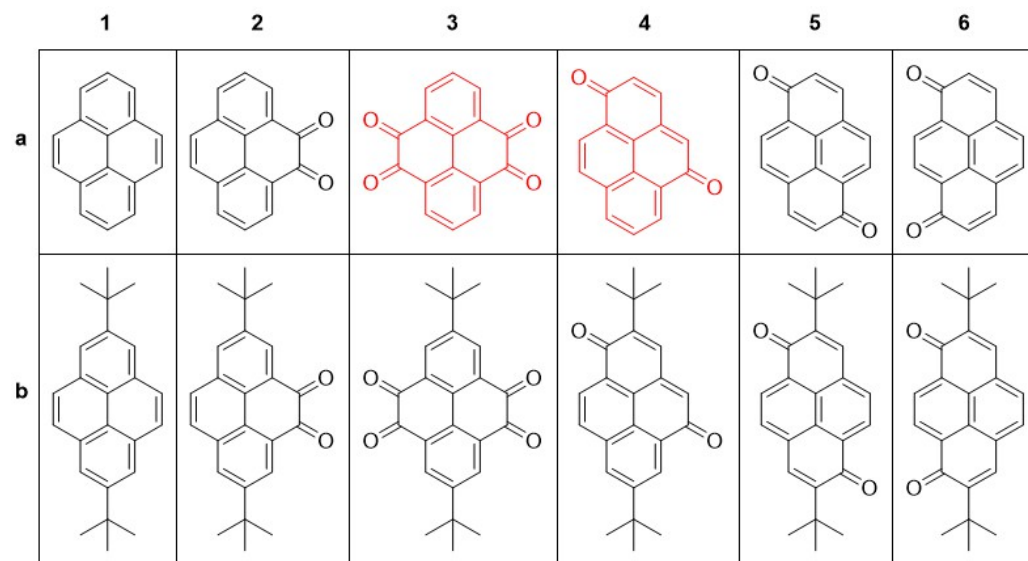


Table S2. Summary of results for the reactions of **1a** and **1b** with the 3 main [O]/S combinations.

Substrate	[O]	S	Temp	Time	Product(s)	Yield
1a	H ₅ IO ₆	EtOH (95%)	Reflux	3 h	7	40%
	HIO ₃	AcOH/H ₂ O (+H ₂ SO ₄)	50 °C	16 h	No reaction	—
	IBX	AcOH/H ₂ O	Reflux	4 h	5a 6a 2a	48% 26% 7%
1b	H ₅ IO ₆	EtOH (95%)	Reflux	1.5-5 h	2b	69-76%
	HIO ₃	AcOH/H ₂ O (+H ₂ SO ₄)	50 °C	16 h	3b	56-60%
	IBX	AcOH/H ₂ O	Reflux	4 h	4b	33%
					5b	13%
6b					9%	
2b	6%					

Table S3. Solvents used in this work.

Solvent	CHEM21 Rank ^a	Class	Solubility of 1b
Water	Recommended	Polar protic	Insoluble at reflux
EtOH	Recommended	Polar protic	Soluble at reflux
^t PrOH	Recommended	Polar protic	Soluble at reflux
EtOAc	Recommended	Polar aprotic	Soluble at reflux
Acetone	Recommended	Polar aprotic	Soluble at reflux
DMSO	Problematic	Polar aprotic	Soluble at 110 °C
MeCN ^b	Problematic	Polar aprotic	Soluble at reflux
AcOH	Problematic	Polar protic, acidic	Soluble at reflux
Toluene	Problematic	Non-polar aromatic	Soluble at 25 °C
Heptane	Problematic	Non-polar hydrocarbon	Soluble at reflux
THF ^b	Problematic	Polar aprotic	Soluble at 25 °C
DCM ^b	Hazardous	Halogenated	Soluble at 25 °C

^a CHEM21 rank for each solvent (greenest on top) from ref. [1]; ^b used because it is associated with the RICO methods (ref.[2,3]).

Table S4. Major (+ minor) products of 100 mg scale reactions using 4 equivalents of each oxidant in different solvents.

Solvent	[O] = NaIO ₄	[O] = HIO ₃	[O] = H ₅ IO ₆
H ₂ O	N.R.	N.R.	N.R.
H ₂ O + H ₂ SO ₄	N.R.	N.R.	N.R.
EtOH	N.R.	2b (+ 3b)	2b
^t PrOH	N.R.	2b	1b (+ 2b)
AcOH	1b (+ 2b)	2b (+ 3b)	2b (+ 3b)
AcOH + H ₂ SO ₄	3b	3b	3b
Acetone	N.R.	N.R.	N.R.
Acetone + H ₂ SO ₄	N.R.	N.R.	N.R.
DMSO	N.R.	N.R.	N.R.
DMSO + H ₂ SO ₄	N.R.	1b (+ 2b)	N.R.
Others (from Table S3)	N.R.	N.R.	N.R.

Table S5. Results of **1b** oxidation as function of oxidant and molar ratio in the polar protic organic solvents on a 100 mg scale.

[O]	Solv.	[O] equiv.	Crude mass ^a	Major ^b	Minor ^b	% yield ^c
HIO ₃	EtOH (95%)	2	B	2b	1b	
		3	B	2b	3b	
		8	C	2b	3b	
	<i>i</i> -PrOH (91%)	2	A	2b	1b	62
		3	A	2b	—	83 ^d
		4	B	2b	—	69
		8	C	2b	—	41
	AcOH (95%)	2	B	2b	1b	
		3	B	2b	3b	
		8	D	3b	2b	
		10	D	3b	—	38 ^e
	H ₅ IO ₆	EtOH (95%)	2	A	2b	—
4			B	2b	—	69
6			C	2b	—	49
<i>i</i> -PrOH (91%)		4	B	1b	2b	
		2	B	2b	3b	
AcOH (95%)		4	C	2b	3b	
		6	F	3b	—	< 10

^a Crude mass (mg): A (> 85), B (71-85), C (56-70), D (40-55), E (21-40), F (< 20); ^b major and minor components identified by crude NMR analysis; ^c % yield of the major product (determined after purification, only in case of an 85+ mg crude mass or in case of single reaction product); ^d potential best conditions to selectively make dione **2b**; ^e potential best conditions to selectively make tetraone **3b**.

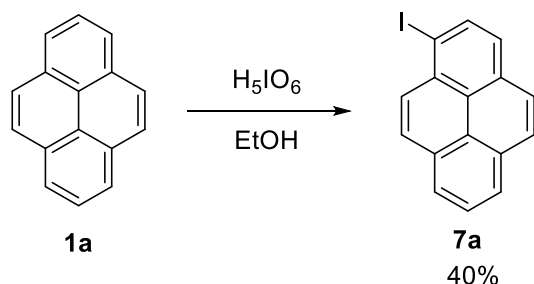
II. General Remarks: Reactions were carried under ambient atmosphere unless otherwise stated. Pyrene, 1,2-benzenediamine, 2-iodobenzoic acid, Oxone[®] monopersulfate, *tert*-butyl chloride, aluminum chloride, sodium metaperiodate, potassium bromide (FT-IR grade) were purchased from Sigma Aldrich. Periodic acid was purchased from Acros Organics. Iodic acid was purchased from Alfa Aesar. Iodic acid and periodic acid were stored in a desiccator in the dark. Freshly recrystallized iodic and periodic acid ensured best reaction outcomes. Iodine was purchased from Fisher Chemical. Potassium bromide was dried at 80 °C under vacuum overnight prior to use for FT-IR. All other chemicals were used as obtained. NMR experiments were performed in chloroform-*d* (D, 99.9% + 0.05% *v/v* TMS) or in dimethylsulfoxide-*d*₆ (D, 99.9%) at 298K using commercial Bruker instrumentation. Chemical shifts were referenced based on the NMR solvent resonance. FT-IR spectra were collected using Nicolet IR100 FT-IR spectrometer. High resolution mass spectrometry was performed using Orbitrap Velos instrument.

III. Synthetic Procedures:

2,7-Di-*tert*-butylpyrene (1b) was synthesized from pyrene (**1a**) according to a literature procedure⁴ in 92% yield after purification by recrystallization from EtOH. ¹H NMR (CDCl₃, 400 MHz): δ 8.18 (s, 4H), 8.01 (s, 4H), 1.58 (s, 18H); ¹³C NMR (CDCl₃, 100 MHz): δ 148.5, 130.8, 127.4, 122.9, 122.0, 35.2, 32.0. Data were identical to reported literature.⁵

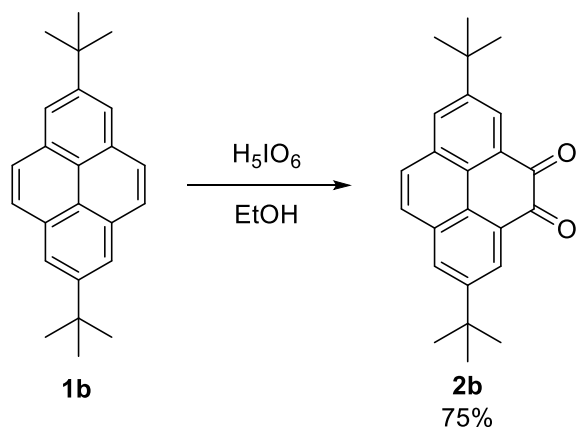
2-Iodoxybenzoic acid (IBX) was synthesized from 2-iodobenzoic acid according to a literature procedure⁶ in 77% yield after purification by washing with water, acetone, and DCM. ¹H NMR (DMSO-d₆, 400 MHz): δ 8.15 (d, J = 7.8 Hz, 1H), 7.97 – 8.06 (m, 2H), 7.84 (t, J = 7.8 Hz, 1H); ¹³C NMR (DMSO-d₆, 100 MHz): δ 167.5, 146.5, 133.4, 132.9, 131.4, 130.1, 125.0. Data were identical to reported literature.⁷

Reactions of 1a with H₅IO₆ and IBX

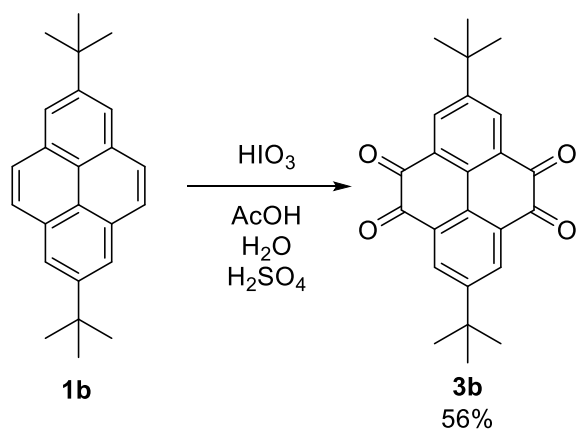


1-Iodopyrene (7). A mixture of **1a** (1.00 g, 4.94 mmol, 1.0 equiv.) and H₅IO₆ (2.25 g, 9.88 mmol, 2.0 equiv.) in EtOH (50 mL, 95%) was maintained at reflux for 3 h. The reaction color changed from pale to dark yellow to red over that period. After complete conversion was confirmed by TLC, the reaction mixture was allowed to cool to RT and poured in an aqueous sodium thiosulfate solution (100 mL, 10%), then cooled in an ice bath for 2 h. A yellow brownish precipitate was collected by vacuum filtration, which was washed with cold water (3 x 100 mL). The solid was purified by flash chromatography (SiO₂, 97:3 heptane/EtOAc) to yield **7** (0.650 g, 1.98 mmol, 40%) as a yellow solid: mp 84–86 °C; ¹H NMR (CDCl₃, 400 MHz): δ 8.50 (d, J = 8.1 Hz, 1H), 8.29 (d, J = 9.2 Hz, 1H), 8.18 – 8.24 (m, 2H), 8.13 (d, J = 9.2 Hz, 1H), 7.99 – 8.11 (m, 3H), 7.86 (d, J = 8.1 Hz, 1H); ¹³C NMR (CDCl₃, 100 MHz): δ 136.7, 132.5, 131.3, 131.0, 130.97, 130.95, 129.3, 127.9, 127.0, 126.4, 125.9, 125.8, 125.6, 125.4, 123.9, 96.2; R_f (SiO₂, 97:3 heptane/EtOAc) = 0.33; IR (KBr, cm⁻¹) 3037, 1584, 1461, 1422, 1375, 1302, 1242, 1178, 1075, 1005, 963, 832, 751, 701. Data were identical to reported in the literature.⁸

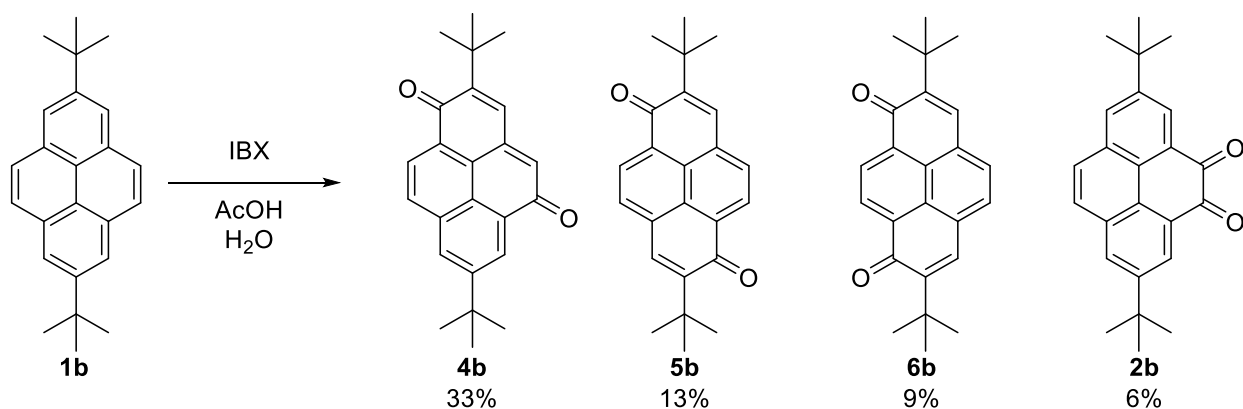
Reactions of **1b** with H_5IO_6 , HIO_3 and IBX



2,7-Di-tert-butylpyrene-4,5-dione (2b). A mixture of **1b** (1.00 g, 3.18 mmol, 1.0 equiv.) and H_5IO_6 (1.81 g, 7.95 mmol, 2.5 equiv.) and EtOH (50 mL, 95%) was maintained at vigorous reflux for 3 h. The reaction color changed from colorless to yellow to orange to red over that period (Fig. S1). After complete conversion was confirmed by TLC, the homogenous dark red reaction mixture was allowed to cool to RT. Compound **2b** slowly crystallized upon cooling. Water (50 mL) was added and aqueous sodium thiosulfate (50 mL, 10%) were successively added and the mixture was stirred in an ice bath for 2 h. The orange precipitate was collected by vacuum filtration and washed with cold water (3 x 100 mL). The crude solid was purified by filtration through a silica plug (9:1 heptane/EtOAc) to remove inorganic contaminants. Solvent was removed under reduced pressure to provide dione **2b** (0.820 g, 2.38 mmol, 75%) as orange solid: mp 240–242 °C (lit.² 241–244 °C); 1H NMR ($CDCl_3$, 400 MHz): δ 8.54 (d, $J = 2.0$ Hz, 2H), 8.12 (d, $J = 2.0$ Hz, 2H), 7.79 (s, 2H), 1.49 (s, 18H); ^{13}C NMR ($CDCl_3$, 100 MHz): δ 181.0 (C_q), 151.1 (C_q), 131.9 (C_q), 131.8 (CH), 129.7 (C_q), 128.35 (CH), 127.3 (CH), 126.5 (C_q), 35.2 (C_q), 31.2 (CH_3) (NMR data were identical to reported literature.^{2, 3}); IR (KBr, ν_{max}) 1672 cm^{-1} ; UV-Vis (EtOH, λ_{max}) 440 nm; HRMS (ESI/Orbitrap) m/z : $[M+H]^+$ Calcd for $C_{24}H_{25}O_2$ 345.1849; Found 345.1835.



2,7-Di-*tert*-butylpyrene-4,5,9,10-tetraone (3b). A mixture of **1b** (1.00 g, 3.18 mmol, 1.0 equiv.), HIO_3 (3.36 g, 19.1 mmol, 6.0 equiv), AcOH (45 mL, 95%), and aqueous H_2SO_4 (0.184 M; 5 mL, 0.92 mmol, 0.3 equiv.) was maintained at 50 °C for 16 h. After complete conversion was confirmed by TLC, the dark orange reaction mixture was allowed to cool to RT and poured in water (ca. 100 mL). The mixture was then cooled in an ice bath for 2 h, and the resultant orange precipitate was collected by vacuum filtration and washed with cold water (3 x 100 mL) and aqueous sodium thiosulfate (100 mL, 10%). The collected precipitate was purified by filtration through a silica plug (4:1 heptane/EtOAc) to remove inorganic contaminants. Solvent was removed under reduced pressure to provide **3b** (0.670 g, 1.79 mmol, 56%) as an orange solid: mp >300 °C (lit.¹⁴ >300 °C); ^1H NMR (CDCl_3 , 400 MHz): δ 8.48 (s, 4H), 1.43 (s, 18H); ^{13}C NMR (CDCl_3 , 100 MHz): δ 178.2 (C_q), 154.8 (C_q), 133.9 (CH), 132.2 (C_q), 130.5 (C_q), 35.4 (C_q), 30.7 (CH_3) (NMR data were identical to reported literature.²); IR (KBr, ν_{max}) 1676 cm^{-1} (lit.¹⁴ 1670 cm^{-1}); UV-Vis (EtOH, λ_{max}) 421 nm (lit.¹⁴ 420 nm); HRMS (ESI/Orbitrap) m/z : $[\text{M}+\text{H}]^+$ Calcd for $\text{C}_{24}\text{H}_{23}\text{O}_4$ 375.1591; Found 375.1580.



2,7-Di-tert-butylpyrene-1,5-dione (4b), 2,7-di-tert-butylpyrene-1,6-dione (5b), 2,7-di-tert-butylpyrene-1,8-dione (6b), and 2,7-Di-tert-butylpyrene-4,5-dione (2b). A mixture of **1b** (100 mg, 0.318 mmol, 1.0 equiv.) and IBX (535 mg, 1.91 mmol, 6.0 equiv.) in AcOH (5 mL, 95%) was maintained at reflux for 4 h. The reaction color changed from colorless to orange to maroon red over that period. After complete conversion was confirmed by TLC, the reaction mixture was allowed to cool to RT, poured into water (ca. 20 mL), and then cooled in an ice bath for 2 h, after which a brick red precipitate was collected by vacuum filtration. The solid was washed with cold water (3 x 10 mL) and purified by column chromatography (SiO₂, 9:1 heptane/EtOAc) to yield **4b**, the major product, as an orange solid (35.8 mg, 0.104 mmol, 33%): mp >300 °C; ¹H NMR (CDCl₃, 500 MHz) δ 8.63 (d, *J* = 2.0 Hz, 1H), 8.21 (d, *J* = 8.7 Hz, 1H), 8.09 (d, *J* = 2.0 Hz, 1H), 8.05 (d, *J* = 8.7 Hz, 1H), 7.28 (d, *J* = 0.7 Hz, 1H), 6.80 (d, *J* = 0.7 Hz, 1H), 1.48 (s, 9H), 1.43 (s, 9H); ¹³C NMR (CDCl₃, 125 MHz) δ 186.2 (C_q), 185.0 (C_q), 152.4 (C_q), 150.9 (C_q), 140.3 (C_q), 135.0 (CH), 133.7 (C_q), 131.6 (CH), 131.15 (CH), 130.55 (CH), 130.25 (C_q), 129.5 (CH), 129.3 (C_q), 125.8 (C_q), 125.6 (C_q), 123.8 (CH), 35.6 (C_q), 35.4 (C_q), 31.0 (CH₃), 29.6 (CH₃); *R_f* (SiO₂, 9:1 heptane/EtOAc) = 0.37; IR (KBr, ν_{max}) 1634 cm⁻¹; UV-Vis (EtOH, λ_{max}) 434 nm; HRMS (ESI/Orbitrap) *m/z*: [M+H]⁺ Calcd for C₂₄H₂₅O₂ 345.1849; Found 345.1844; [2M+Na]⁺ Calcd for C₄₈H₄₈O₄Na 711.3445; Found 711.3444. Additional characterization data for **4b** is shown below. Diones **5b**, **6b** and **2b** were isolated as minor products. **5b** was isolated as an orange solid (14.2 mg, 0.0412 mmol, 13%): mp >300 °C; ¹H NMR (CDCl₃, 500 MHz) δ 8.43 (d, *J* = 7.6 Hz, 2H), 7.74 (d, *J* = 7.6 Hz, 2H), 7.51 (s, 2H), 1.44 (s, 18H); ¹³C NMR (CDCl₃, 125 MHz) δ 185.3 (C_q), 149.9 (C_q), 135.4 (CH), 134.0 (C_q), 130.75 (CH), 130.4 (C_q), 130.0 (CH), 126.1 (C_q), 35.4 (C_q), 29.4 (CH₃); *R_f* (SiO₂, 9:1 heptane/EtOAc) = 0.39; IR (KBr, ν_{max}) 1619 cm⁻¹; UV-Vis (EtOH, λ_{max}) 443 nm. Data were identical to reported literature.¹⁴ **6b** was isolated as a red solid (9.5 mg, 0.028 mmol, 9%): mp 280–283 °C; ¹H NMR (CDCl₃, 400 MHz) δ 8.59 (s, 2H), 7.57 (s,

2H), 7.50 (s, 2H), 1.44 (s, 18H); R_f (SiO₂, 9:1 heptane/EtOAc) = 0.33; IR (KBr, ν_{\max}) 1627 cm⁻¹; UV-Vis (EtOH, λ_{\max}) 487 nm. Data were identical to reported literature.¹⁴ **2b** was isolated as an orange solid (6.5 mg, 0.019 mmol, 6%). Characterization data obtained were identical to that reported above.

Characterization of 4b:

Dione **4b** is previously unreported. The structure of this compound was assigned by a combination of HRMS, UV-Vis, FT-IR, and NMR analysis (¹H, ¹³C, DEPT-135, DEPT-90, ¹H-¹H ROESY, and ¹H-¹³C HSQC).

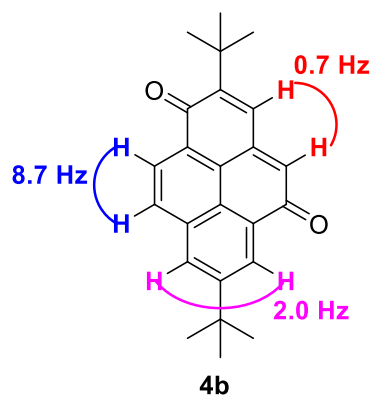
The mass obtained by HRMS is consistent with the assigned structure with mass error <1.5 ppm.

An intense strong carbonyl stretching peak in the IR spectrum at 1634 cm⁻¹ is consistent with the carbonyl stretching of other pyrene diones possessing non-adjacent carbonyl groups (i.e. [1615–1640 cm⁻¹], Table S6).

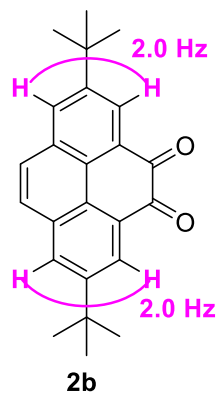
Pyrene diones have a characteristic (n- π^*)^{13, 14} electronic transition within the [violet-blue-green] absorption range responsible of their intense color [yellow-orange-red] under ambient light.

Compound **4b** exhibits this characteristic n- π^* electronic transition at 434 nm.

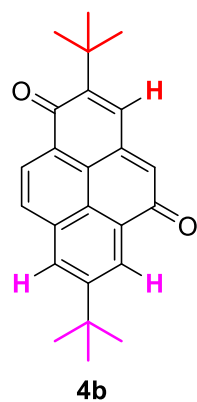
The one-dimensional ¹H NMR exhibits 3 sets of doublets integrating to 2H each with 3 different coupling constants, $J = 8.7, 2.0,$ and 0.7 Hz, which are consistent with *ortho*-aromatic coupling, *meta*-aromatic coupling, and dienyllic coupling, respectively, as shown in the structure below. In addition, 2 singlets integrating to 9H each were observed in the aliphatic region, consistent with 2 non-equivalent *tert*-butyl groups.



The 2.0 Hz coupling is consistent with the *meta*-aromatic coupling of the two aromatic protons separated by the *tert*-butyl group in **2b**.



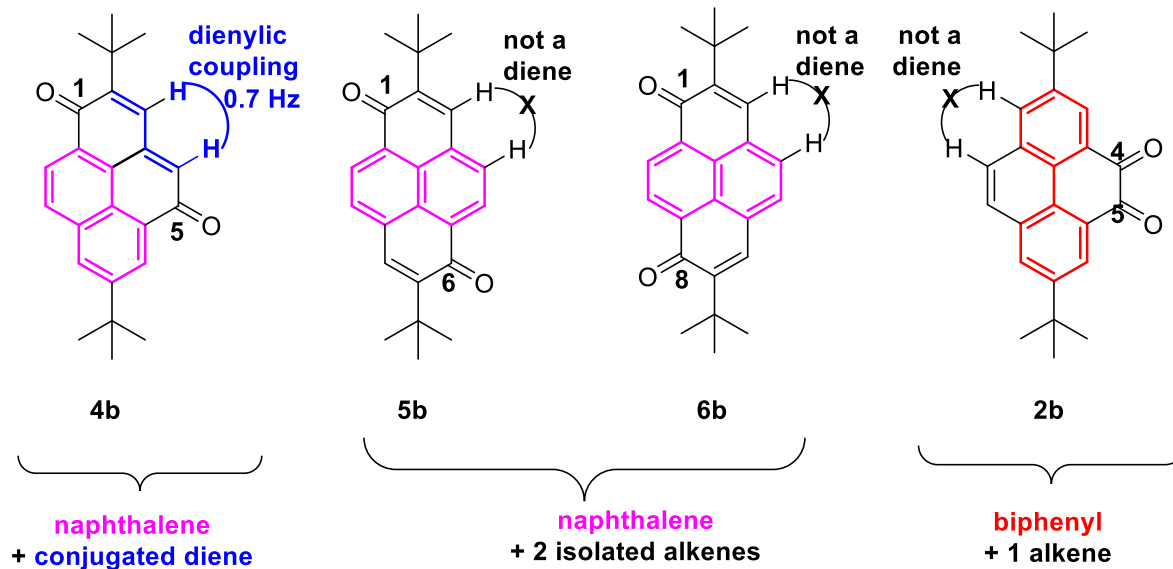
The two-dimensional ROESY spectrum of **4b** revealed that one *tert*-butyl group has two neighboring *ortho*-protons (the two doublets with *meta*-aromatic coupling) whereas the other *tert*-butyl has just one neighboring *ortho*-proton (one of the two doublets with dienylic coupling) as shown below.



The one-dimensional ^{13}C NMR spectrum exhibits 2 non-equivalent carbonyl peaks (185–187 ppm), 14 peaks in the sp^2 -hybridized region (123–153 ppm), and 4 peaks in the aliphatic region corresponding to the non-equivalent *tert*-butyl groups (29–36 ppm).

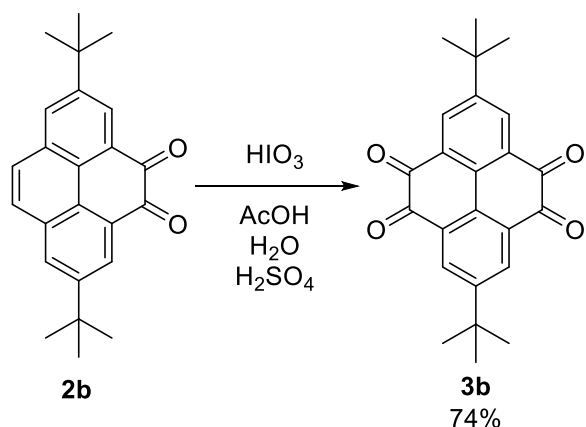
The DEPT-135 and DEPT-90 spectra indicate that 6 out of the 14 sp^2 -hybridized carbons are =CH and 2 out of the 4 sp^3 -hybridized are $-\text{CH}_3$. The two-dimensional HSQC spectrum allowed us to correlate the six =CH and the two $-\text{CH}_3$ carbon peaks to their corresponding proton peaks.

The aromatic core in diones **4b-6b** consists of two fused rings **with 10 conjugated π -electrons in total (i.e. naphthalene/one Clar sextet)** as opposed to dione **2b** that possesses **two separate rings with 6 conjugated π -electrons each (i.e. biphenyl/two Clar sextets)**. Diones **4b**, **5b** and **6b** all possess 2 alkene bonds. In dione **4b**, unlike **5b** and **6b**, the two alkene bonds form a **conjugated diene**. This is consistent with the **dienylic (0.7 Hz) coupling of the diene protons** observed in the ^1H NMR of **4b**.



Other reactions:

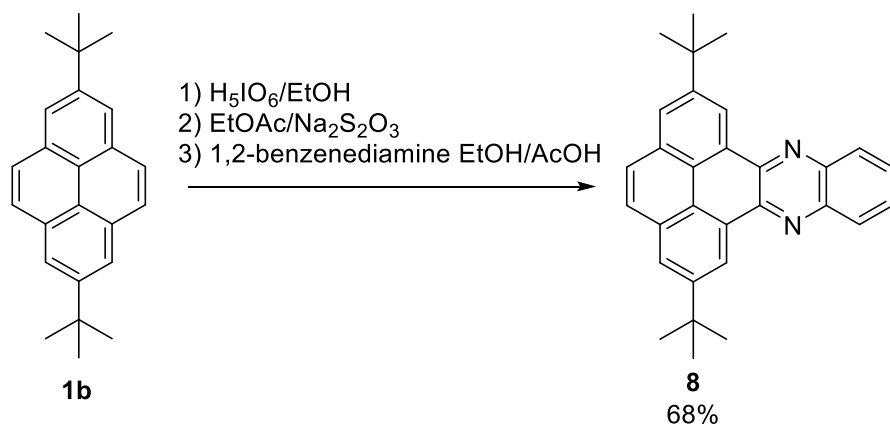
3b from 2b



2,7-Di-tert-butylpyrene-4,5,9,10-tetraone (3b). A mixture of **2b** (100 mg, 0.290 mmol, 1.0 equiv.) and HIO₃ (153 mg, 0.870 mmol, 3.0 equiv) in AcOH (4.5 mL, 95%), and aqueous H₂SO₄ (0.184 M; 0.5 mL, 0.092 mmol, 0.3 equiv.) was maintained at 50 °C for 16 h. After complete conversion was confirmed by TLC, the dark orange reaction mixture was allowed to cool to RT and poured in water (ca. 10 mL). The mixture was then cooled in an ice bath for 2 h, and the resultant orange precipitate was collected by vacuum filtration and washed with cold water (3 x 10 mL) and aqueous sodium thiosulfate (10 mL, 10%). The collected precipitate was purified by filtration through a silica plug (4:1 heptane/EtOAc) to remove inorganic contaminants. Solvent was removed under reduced pressure to provide **3b** (80.0 mg, 0.214 mmol, 74%) as an orange solid. Characterization data obtained were identical to that reported above.

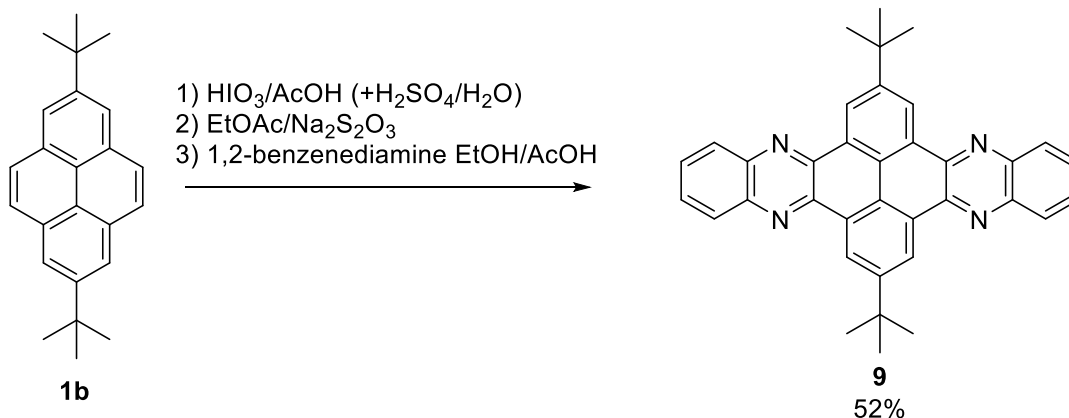
Direct synthesis of *N*-heteroacenes **8** and **9** from **1b**:

Via crude **2b**



2,7-Di-*tert*-butylphenanthro[4,5-*abc*]phenazine (8). A mixture of **1b** (100 mg, 0.318 mmol, 1.0 equiv.) and H_5IO_6 (145 mg, 0.636 mmol, 2.0 equiv.) and EtOH (5 mL, 95%) was maintained at reflux for 1.5 h. The reaction color changed from colorless to yellow to orange to red over that period (Fig. S1). After complete conversion was confirmed by TLC, the homogenous dark red reaction mixture was allowed to cool to RT and poured in water (ca. 50 mL), extracted with ethyl acetate (3 x 10 mL). The combined organic layer was washed with aqueous sodium thiosulfate (10 mL, 10%) then brine (10 mL), dried over MgSO_4 , and filtered. Following the removal of solvents under reduced pressure, crude **2b** was dissolved in EtOH (5 mL) and added to a solution of 1,2-benzenediamine (51.6 mg, 0.477 mmol, 1.5 equiv.) in glacial AcOH (5 mL). The mixture was purged with argon for 10 minutes and maintained at reflux for 3h under inert atmosphere, after which it was allowed to cool to RT and placed in an ice bath for 1h. A yellow precipitate was collected by vacuum filtration. The crude solid was washed with cold AcOH (10 mL), water (3 x 20 mL) then cold EtOH (3 x 10 mL) and allowed to dry to provide compound **8** (90.2 mg, 0.216 mmol, 68% over 2 steps) as yellow solid (Fig. S3): mp $>300\text{ }^\circ\text{C}$; $^1\text{H NMR}$ (CDCl_3 , 400 MHz): δ 9.66 (d, $J = 1.9\text{ Hz}$, 2H), 8.40 – 8.44 (m, 2H), 8.28 (d, $J = 1.9\text{ Hz}$, 1H), 8.00 (s, 2H), 7.86 – 7.90 (m, 2H), 1.68 (s, 18H); $^{13}\text{C NMR}$ (CDCl_3 , 100 MHz): δ 149.7, 143.8, 142.2, 131.2, 129.6, 129.5, 129.0, 127.3, 125.8, 124.3, 121.5, 35.5, 31.9; IR (KBr, cm^{-1}) 3057, 2956, 1709, 1613, 1515, 1470, 1356, 1258, 1225, 1108, 1011, 885, 803, 757, 720; UV-Vis (EtOH, λ_{max}) 436 nm. Data were identical to reported literature.¹⁵

Via crude 3b



2,11-Di-tert-butylquinoxalino[2',3':9,10]phenanthro[4,5-abc]phenazine (9). A mixture of **1b** (100 mg, 0.318 mmol, 1.0 equiv.), HIO₃ (336 mg, 1.91 mmol, 6.0 equiv.), AcOH (4.5 mL, 95%) and aqueous H₂SO₄ (0.184 M; 0.5 mL, 0.092 mmol, 0.3 equiv.) was maintained at 50 °C for 16 h. After complete conversion was confirmed by TLC, the dark orange reaction mixture was allowed to cool to RT and poured in water (ca. 50 mL), extracted with ethyl acetate (3 x 10 mL). The combined organic layer was washed with water (3 x 25 mL) aqueous sodium thiosulfate (25 mL, 10%) then brine (25 mL), dried over MgSO₄, and filtered. Following the removal of solvents under reduced pressure, crude **3b** was dissolved in EtOH (5 mL) and added to a solution of 1,2-benzenediamine (103 mg, 0.954 mmol, 3.0 equiv.) in glacial AcOH (5 mL). The mixture was purged with argon for 10 minutes and maintained at reflux for 3 h under inert atmosphere. The reaction was allowed to cool to RT and placed in an ice bath for 1 h. A yellow precipitate was collected by vacuum filtration. The crude solid was washed with cold AcOH (15 mL), water (3 x 25 mL) then cold EtOH (3 x 15 mL) and allowed to dry to provide compound **9** (86.0 mg, 0.166 mmol, 52% over 2 steps) as yellow solid: mp >300 °C; ¹H NMR (CDCl₃, 400 MHz) δ 9.82 (s, 4H), 8.43 – 8.47 (m, 4H), 7.89 – 7.94 (m, 4H), 1.77 (s, 18H); IR (KBr, cm⁻¹) 3064, 2949, 1930, 1827, 1728, 1611, 1538, 1455, 1337, 1238, 1108, 1017, 883, 742; UV-Vis (DCM, λ_{max}) 414 nm. Data were identical to reported literature.¹⁵

The very first I₂/HIO₃ iodination attempt:

A mixture of **1b** (1.00 g, 3.18 mmol, 1.0 equiv.), I₂ (1.78 g, 7.00 mmol, 2.2 equiv.), HIO₃ (0.616 g, 3.50 mmol, 1.1 equiv) and glacial AcOH (50 mL) was maintained at reflux for 16 h. The reaction mixture was allowed to cool to RT and poured in water (ca. 100 mL), extracted with DCM (5 x 30 mL). The combined organic layer was washed with aqueous sodium thiosulfate (3 x 25 mL, 10%) and brine (3 x 25 mL), dried over MgSO₄ and filtered. Solvents were removed under reduced pressure. The dark orange residue consisted of a mixture of **2b** and unreacted **1b** by NMR analysis. The crude solid was purified by flash chromatography (SiO₂, 9:1 heptane/EtOAc). Dione **2b** (0.658 g, 1.91 mmol, 60%) was isolated as orange solid. Characterization data obtained were identical to that reported above.

Optimization of reaction conditions:

Different oxidants/solvents (Table S4)

A mixture of **1b** (100 mg, 0.318 mmol, 1.0 equiv.), oxidant (1.27 mmol, 4.0 equiv.), solvent (5 mL) was maintained at reflux (or 110 °C for DMSO) until complete conversion was confirmed by TLC (otherwise for 16 h). The reaction mixture was then allowed to cool to RT and poured in water (ca. 50 mL).

For water and water-miscible solvents: the mixture was cooled in ice for 2 h and the crude product was collected by vacuum filtration. The crude solid was washed with water (3 x 50 mL), aqueous sodium thiosulfate (50 mL, 10%), and allowed to dry.

For water-immiscible solvents: the mixture was extracted with ethyl acetate (3 x 10 mL). The combined organic layer was washed with aqueous sodium thiosulfate (50 mL, 10%), brine (50 mL), dried over MgSO₄, and filtered. Solvents were removed under reduced pressure.

The reaction outcome was then evaluated by TLC and by ¹H NMR analysis.

Different molar ratios of oxidants (Table S5)

A mixture of **1b** (100 mg, 0.318 mmol, 1.0 equiv.), oxidant (as indicated), solvent (5 mL) was maintained at reflux until complete conversion was confirmed by TLC (otherwise for 6 h). The reaction mixture was then allowed to cool to RT and poured in water (ca. 50 mL) and cooled in ice for 2 h, after which the crude product was collected by vacuum filtration. The crude solid was washed with water (3 x 50 mL), aqueous sodium thiosulfate (50 mL, 10%), and allowed to dry, and the crude mass was determined. The crude products were then evaluated by TLC and by ¹H NMR analysis. The yield of the major product (wherever reported) was determined following chromatographic purification.

Scaling up (Table 1)

A mixture of **1b** (1.0 equiv.), H₅IO₆ (2.0 equiv.), ethanol (50 mL/g, 95%) was maintained at reflux and the reaction progress was monitored by TLC. Increments of H₅IO₆ (0.5 equiv.) were added as needed until complete conversion was achieved. The reaction mixture was then allowed to cool to RT and poured in water (50 mL/g) and worked up as described above. The crude products were then evaluated by TLC and by ¹H NMR analysis. The yield of **2b** was determined following chromatographic purification.

IV. Summary of Characterization Data:

Table S6. Summary of the main characterization data collected for the oxidation derivatives in this work and literature references (if available).

#	¹ H NMR (CDCl ₃)	mp, °C	IR (KBr, ν _{C=O}), cm ⁻¹	UV-Vis (EtOH, n-π*), nm	Lit.
2a	8.49 (dd, <i>J</i> = 7.4, 1.1 Hz, 2H) 8.18 (dd, <i>J</i> = 8.0, 1.1 Hz, 2H) 7.85 (s, 2H) 7.76 (t, <i>J</i> = 7.7 Hz, 2H)	>300	1667	419	NMR ³ mp ³ IR ¹² UV-Vis ¹³
2b	8.54 (d, <i>J</i> = 2.0 Hz, 2H) 8.12 (d, <i>J</i> = 2.0 Hz, 2H) 7.79 (s, 2H) 1.49 (s, 18H)	240-242	1672	440	NMR ² mp ²
3b	8.48 (s, 4H) 1.43 (s, 18H)	>300	1676	421	NMR ^{2, 14} mp ^{2, 14} IR ^{14, 16} UV-Vis ¹⁴
4b	8.63 (d, <i>J</i> = 2.0 Hz, 1H) 8.21 (d, <i>J</i> = 8.7 Hz, 1H) 8.09 (d, <i>J</i> = 2.0 Hz, 1H) 8.05 (d, <i>J</i> = 8.7 Hz, 1H) 7.28 (d, <i>J</i> = 0.7 Hz, 1H) 6.80 (d, <i>J</i> = 0.7 Hz, 1H) 1.48 (s, 9H) 1.43 (s, 9H)	>300	1634	434	N/A
5a	8.49 (d, <i>J</i> = 7.5 Hz, 2H) 7.84 (d, <i>J</i> = 7.5 Hz, 2H) 7.69 (d, <i>J</i> = 9.8 Hz, 2H) 6.71 (d, <i>J</i> = 9.8 Hz, 2H)	>300	1633	427	NMR ¹⁰ mp ⁹ IR ¹¹ UV-Vis ¹⁰
5b	8.43 (d, <i>J</i> = 7.6 Hz, 2H) 7.74 (d, <i>J</i> = 7.6 Hz, 2H) 7.51 (s, 2H) 1.44 (s, 18H)	>300	1619	443	NMR ¹⁴ mp ¹⁴ IR ¹⁴ UV-Vis ¹⁴
6a	8.66 (s, 2H) 7.68 (s, 2H) 7.68 (d, <i>J</i> = 9.8 Hz, 2H) 6.69 (d, <i>J</i> = 9.8 Hz, 2H)	270-271	1632	457	NMR ¹⁰ mp ⁹ IR ¹¹ UV-Vis ¹⁰
6b	8.59 (s, 2H) 7.57 (s, 2H) 7.50 (s, 2H) 1.44 (s, 18H)	280-283	1627	487	NMR ¹⁴ mp ¹⁴ IR ¹⁴ UV-Vis ¹⁴

Table S7. Complete list of IR absorption bands for all compounds successfully synthesized in this work and literature references (if available).

#	ν [700-3100] (cm ⁻¹), KBr	Lit. IR
1b	3041, 2954, 1598, 1454, 1359, 1215, 1142, 916, 877, 802, 712.	Lit. ⁵ IR
2a	3067, 2923, 2855, 1667, 1610, 1515, 1427, 1348, 1264, 1171, 1063, 1028, 884, 837, 771, 705.	Lit. ¹² IR
2b	3056, 2960, 1672, 1615, 1518, 1467, 1399, 1363, 1226, 1086, 897, 847, 798, 716.	N/A
3b	2960, 1676, 1547, 1423, 1363, 1311, 1262, 1230, 1097, 1020, 915, 833, 719.	Lit. ^{14, 16} IR
4b	3057, 2950, 1722, 1634, 1585, 1465, 1375, 1266, 1111, 1039, 907, 780, 706.	N/A
5a	3045, 2923, 2855, 1633, 1549, 1504, 1435, 1347, 1267, 1179, 1093, 1027, 808, 750.	Lit. ¹¹ IR
5b	2944, 1619, 1542, 1464, 1354, 1239, 1126, 907, 791, 733.	Lit. ¹⁴ IR
6a	3043, 2924, 2861, 1632, 1563, 1450, 1368, 1265, 1176, 1105, 804, 735.	Lit. ¹¹ IR
6b	2397, 1721, 1627, 1568, 1464, 1366, 1251, 1094, 913, 793.	Lit. ¹⁴ IR
7	3037, 1584, 1461, 1422, 1375, 1302, 1242, 1178, 1075, 1005, 963, 832, 751, 701.	Lit. ⁸ IR
8	3057, 2956, 1709, 1613, 1515, 1470, 1356, 1258, 1225, 1108, 1011, 885, 803, 757, 720.	Lit. ¹⁵ IR
9	2960, 1676, 1547, 1423, 1363, 1311, 1262, 1230, 1097, 1020, 915, 833, 719.	Lit. ^{14, 16} IR

Table S8. Retention factor (R_f) values on silica plate of iodination/oxidation derivatives isolated from each reaction.

Substrate	Reagent	Product(s)	Eluent (Vol% EtOAc/heptane)	d_{spot} (cm)	d_{solv} (cm)	R_f
1a	H ₅ IO ₆	7	3%	1.3	4.0	0.33
	HIO ₃	No reaction	--	--	--	--
	IBX	2a	40%	2.1	4.2	0.50
		5a	40%	1.3	4.2	0.31
6a		40%	1.0	4.2	0.24	
1b	H ₅ IO ₆	2b	10%	1.3	4.4	0.30
	HIO ₃	3b	10%	0.2	4.0	0.05
	IBX	5b	10%	1.8	4.6	0.39
		4b	10%	1.7	4.6	0.37
		6b	10%	1.5	4.6	0.33
		2b	10%	1.4	4.6	0.30

V. Visual Aids:

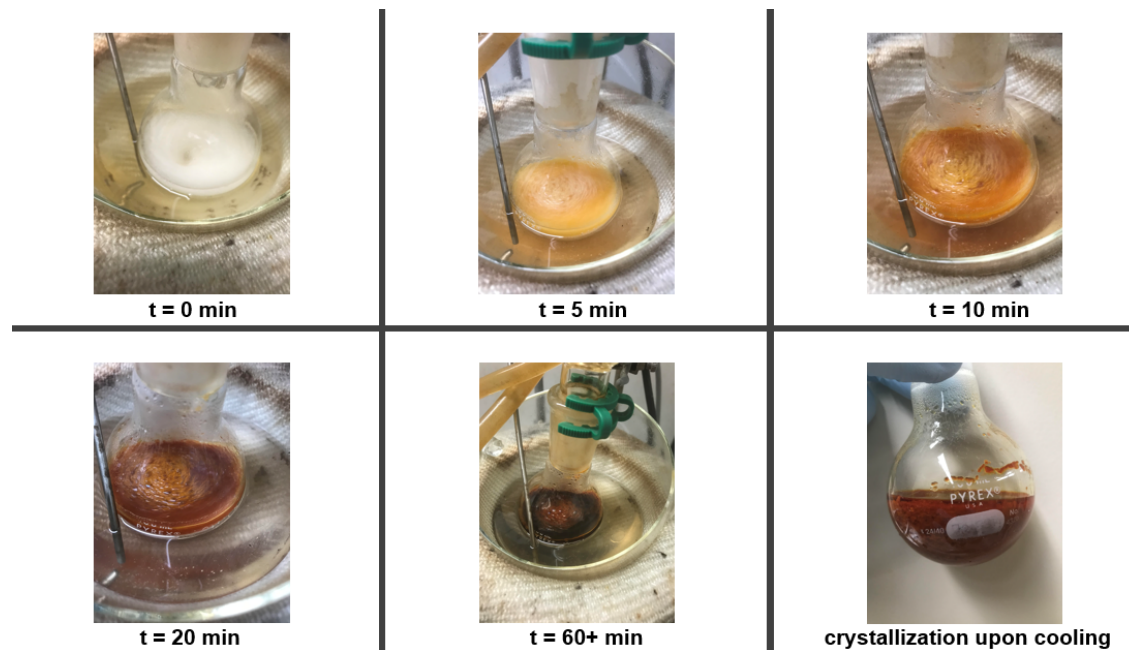


Fig. S1. Color changes throughout the **1b**-H₅IO₆ reaction.



Fig. S2. Crude **2b** (left) made using HIO₃/*i*-PrOH conditions and (right) made using RICO.



Fig. S3. Crude **8** (left) crystallizing upon cooling the reaction mixture and (right) isolated by vacuum filtration.



Fig. S4. TLC comparison (SiO₂, 9:1 heptane/EtOAc) under UV light of crude **2b** (left) made using our optimized conditions and (right) made using RICO.

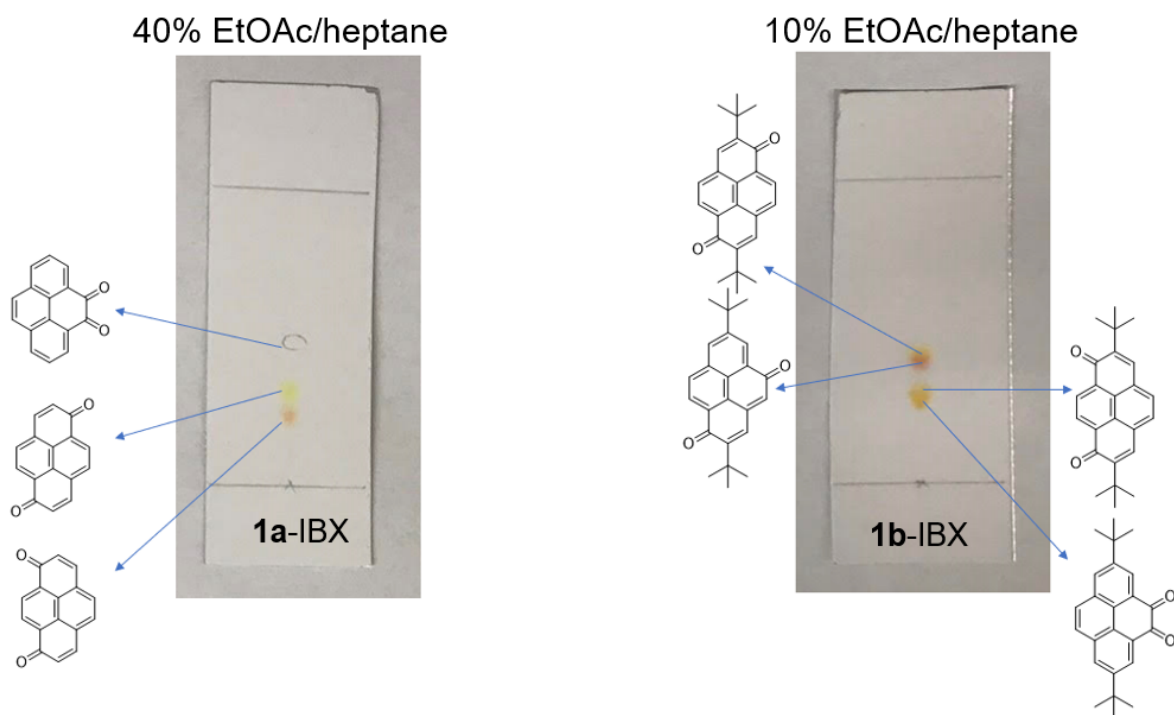
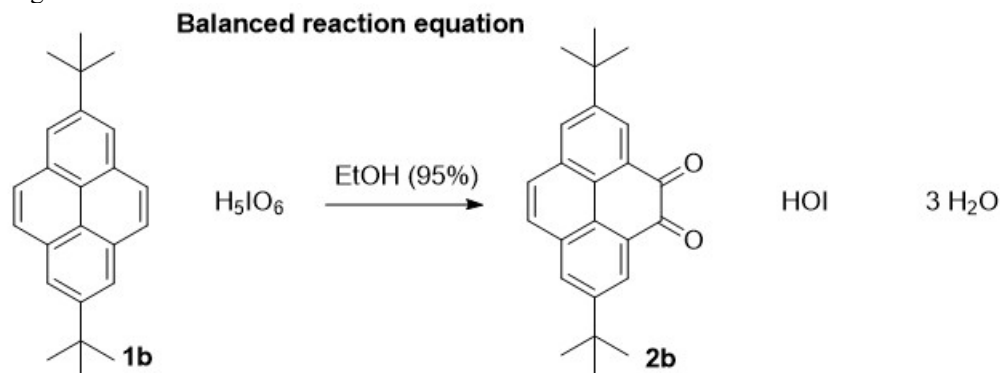


Fig. S5. TLC of the crude (left) **1a-IBX** and (right) **1b-IBX** in the corresponding eluent under ambient light.

VI. Green Chemistry Metrics:

Balanced reaction equation is given based on the postulated mechanism.
EcoScale¹⁷ and (AE, RME, CE)¹⁸ were calculated according to the cited literature.

Table S9. Using the H₅IO₆/EtOH method.



	1b (C ₂₄ H ₂₆)	H ₅ IO ₆	2b (C ₂₄ H ₂₄ O ₂)	HOI	H ₂ O	Sum reactants
experimental mass (g)	1.00	1.81	0.820	---	---	2.81
MW (g/mol)	314.47	227.94	344.45	143.91	18.02	542.41

Atom Economy (AE) = 100.(MW desired product)/(MW all reactants) = 63.5% (vs. 28.8% for the previous methods, see below)

Reaction Mass efficiency (RME) = 100.(mass isolated product)/(mass all reactants) = 29.2% (vs. 11.8% for the previous methods, see below)

Carbon Efficiency (CE) = 100.(#C desired product)/(#C all reactants) = 100%

EcoScale = 100 - penalty points (to make 10 mmol of product)

penalty points:

1- Yield: (100-70)/2 = **15 pts** (assuming a yield of 70%)

2- Price of reaction components: 4.49 g of 1b, 8.13 g of H₅IO₆, 225 mL of 95% EtOH

Estimated price of reagents: 1b (\$1/gram), H₅IO₆ (\$2.5/gram), EtOH (\$0.01/mL)

\$4.49 (1b) + \$20.33 (H₅IO₆) + \$2.25 (EtOH) = \$27.07 (> \$10, < \$50): 3 pts

3- Safety: ethanol (highly flammable): **5 pts**

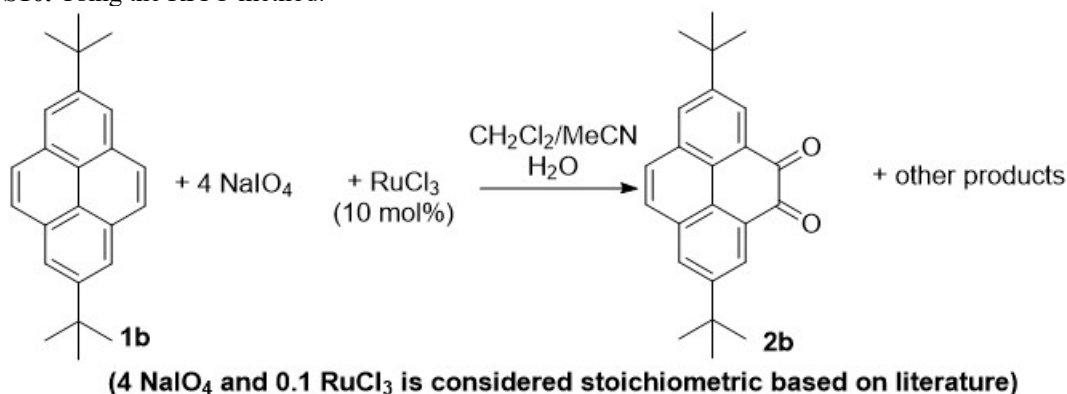
4- Common reaction setup: **0 pt**

5- Heating > 1 h: **3 pts**

6- Workup: cooling to RT, crystallization/filtration (over silica): **1 pt**

EcoScale = 100 - 27 = 73% (vs. 44% for the previous methods, see below)

Table S10. Using the RICO method.



From Ref [2]	1b (C ₂₄ H ₂₆)	NaIO ₄	RuCl ₃ ·3H ₂ O	2b (C ₂₄ H ₂₄ O ₂)	Sum reactants
experimental mass (g)	3.14 (10 mmol)	10.0	0.200	1.58 (46%)	13.34
MW (g/mol)	314.47	213.89	261.47	344.45	1196.18

Atom Economy (AE) = 100.(MW desired product)/(MW all reactants) = 28.8%

Reaction Mass efficiency (RME) = 100.(mass isolated product)/(mass all reactants) = 11.8%

Ecoscale = 100 - penalty points (to make 10 mmol of product)

penalty points:

1- Yield: (100-46)/2 = **27 pts**

2- Price of reaction components:

6.84 g of 1b, 21.8 g of NaIO₄, 0.44 g RuCl₃, 90 mL of MeCN, 90 mL CH₂Cl₂, 110 mL H₂O

Estimated price of reagents:

1b (\$1/gram), NaIO₄ (\$2/gram), RuCl₃·3H₂O (\$48/gram), organic solvents (\$0.01/mL)

\$6.84 (1b) + \$43.60 (NaIO₄) + \$21.12 (RuCl₃) + \$1.80 (MeCN/CH₂Cl₂) = \$73.36 (> \$50): **5 pts**

3- Safety: acetonitrile (highly flammable), dichloromethane (toxic): **10 pts**

4- Common reaction setup: **0 pt**

5- Room temp. < 24 h: **1 pt**

6- Workup: liquid-liquid extraction, classical chromatography : **13 pts**

Ecoscale = 100 - 56 = 44%

VII. NMR Spectra:

1a-H₅IO₆ reaction

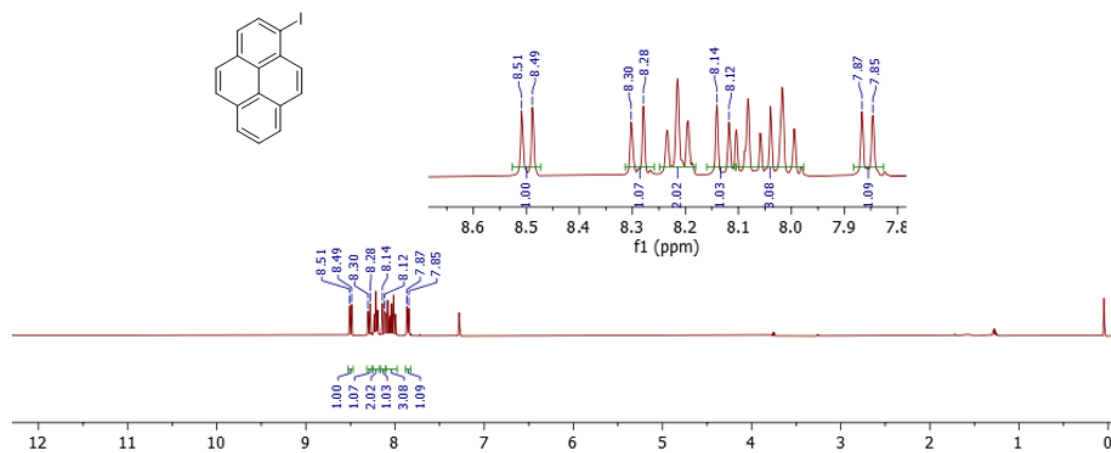


Fig. S6. ¹H NMR in CDCl₃ at 400 MHz of **7** isolated from the **1a-H₅IO₆** reaction.

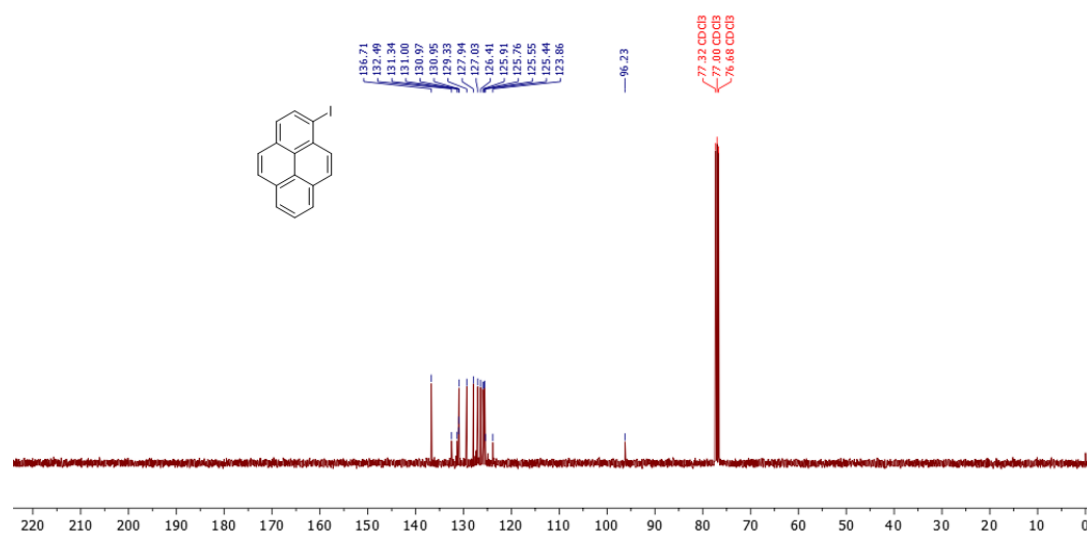


Fig. S7. ¹³C NMR in CDCl₃ at 100 MHz of **7** isolated from the **1a-H₅IO₆** reaction.

1a-IBX reaction

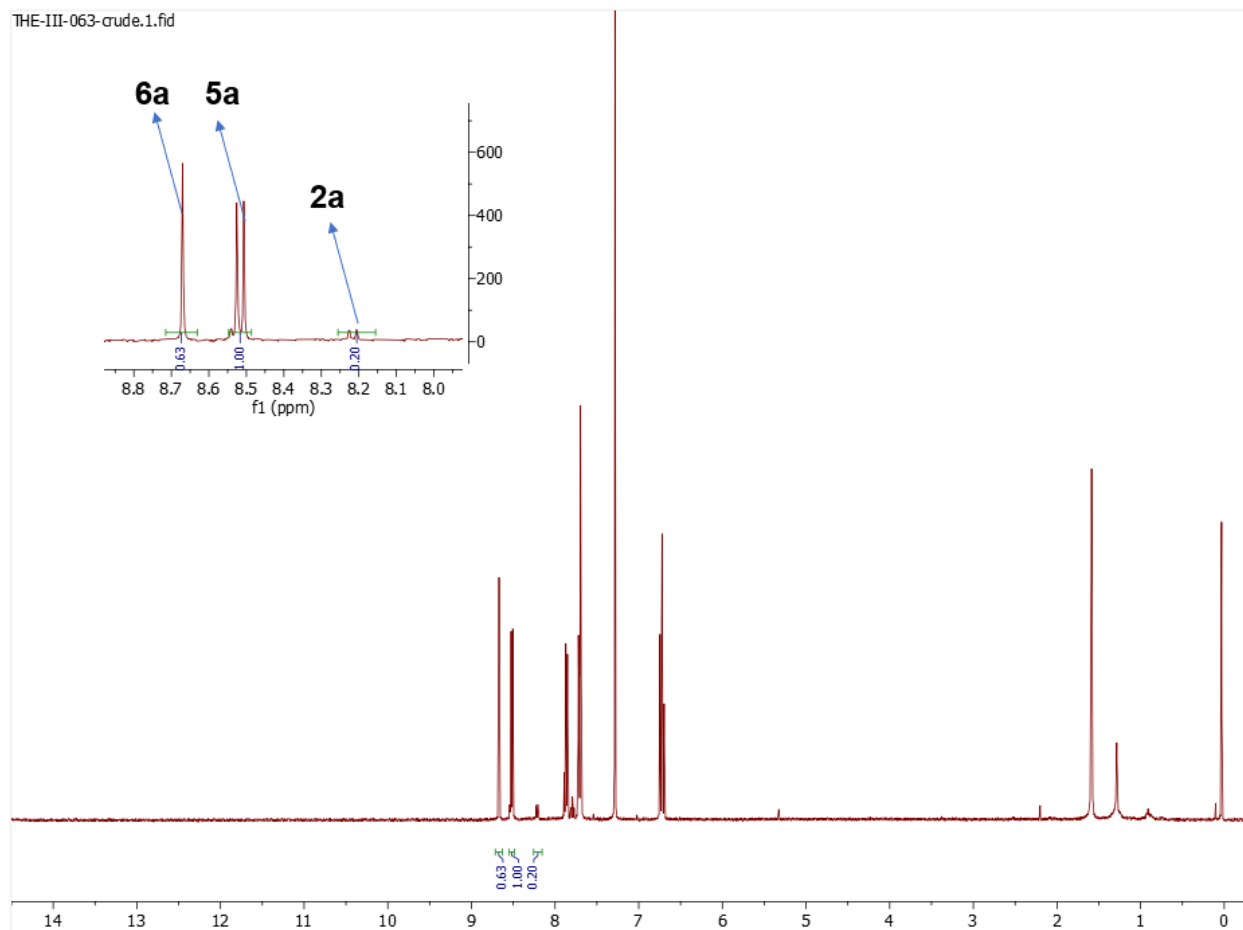


Fig. S8. ^1H NMR in CDCl_3 at 400 MHz of the crude product from the **1a**-IBX reaction.

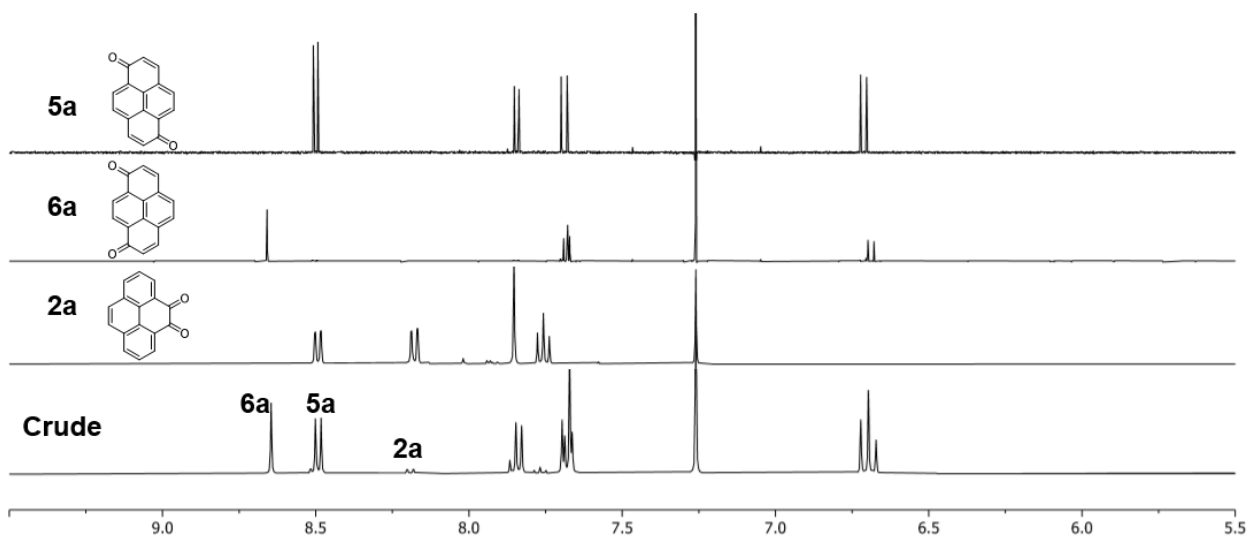


Fig. S9. ^1H NMR spectra of all isolated diones from the **1a**-IBX reaction vs. the crude (decreasing yield from top downwards).

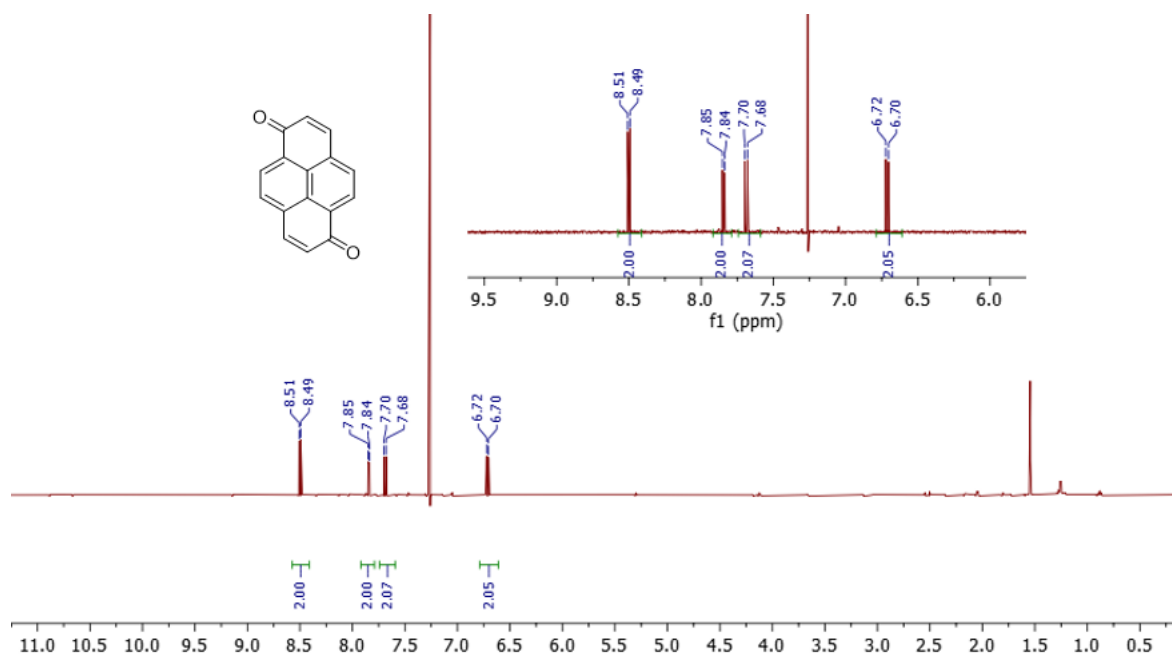


Fig. S10. ¹H NMR in CDCl₃ at 500 MHz of **5a** isolated as major product from the **1a**-IBX reaction.

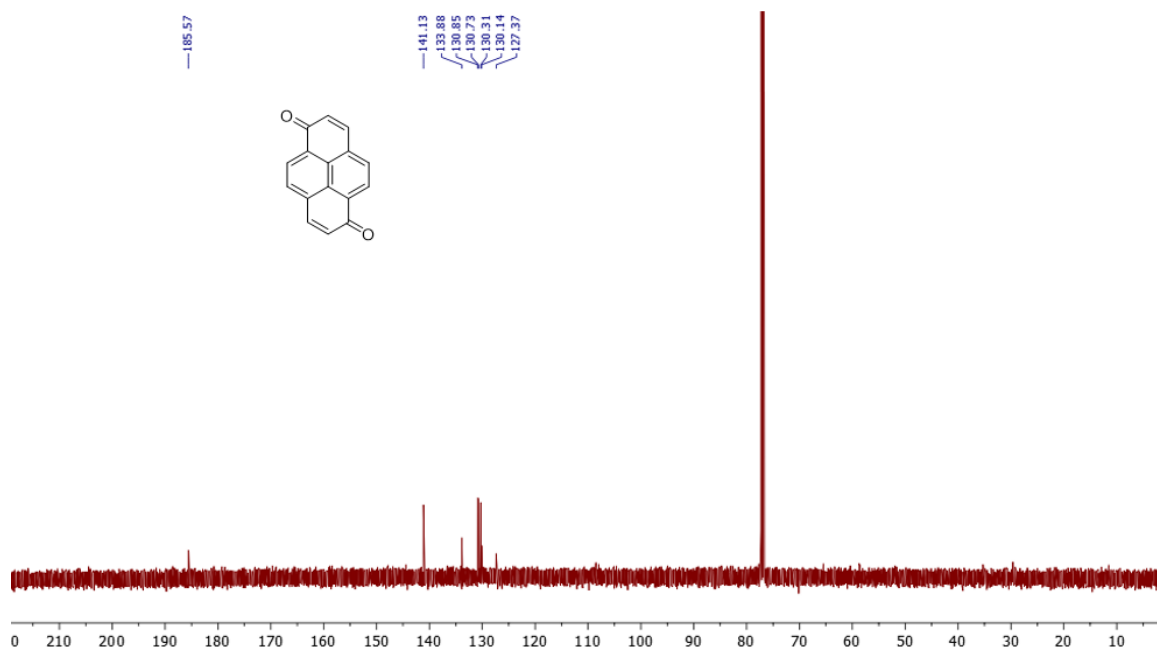


Fig. S11. ¹³C NMR in CDCl₃ at 125 MHz of **5a** isolated as major product from the **1a**-IBX reaction.

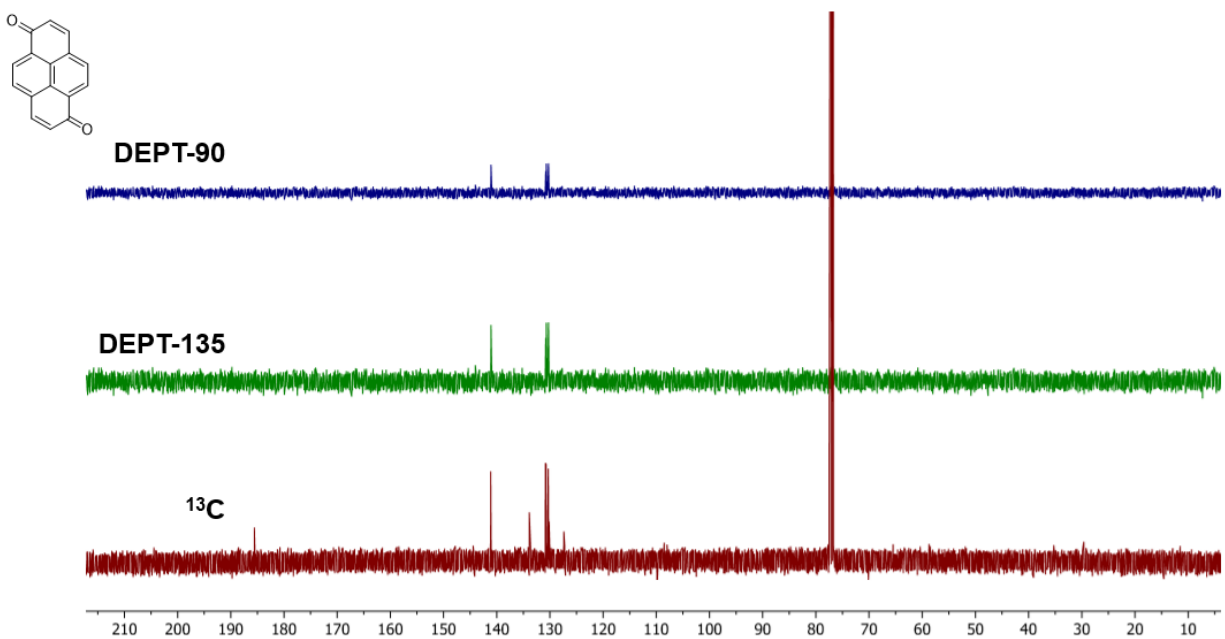


Fig. S12. ^{13}C NMR of **5a** in CDCl_3 at 125 MHz (**red**), DEPT-135 (**green**) and DEPT-90 (**blue**).

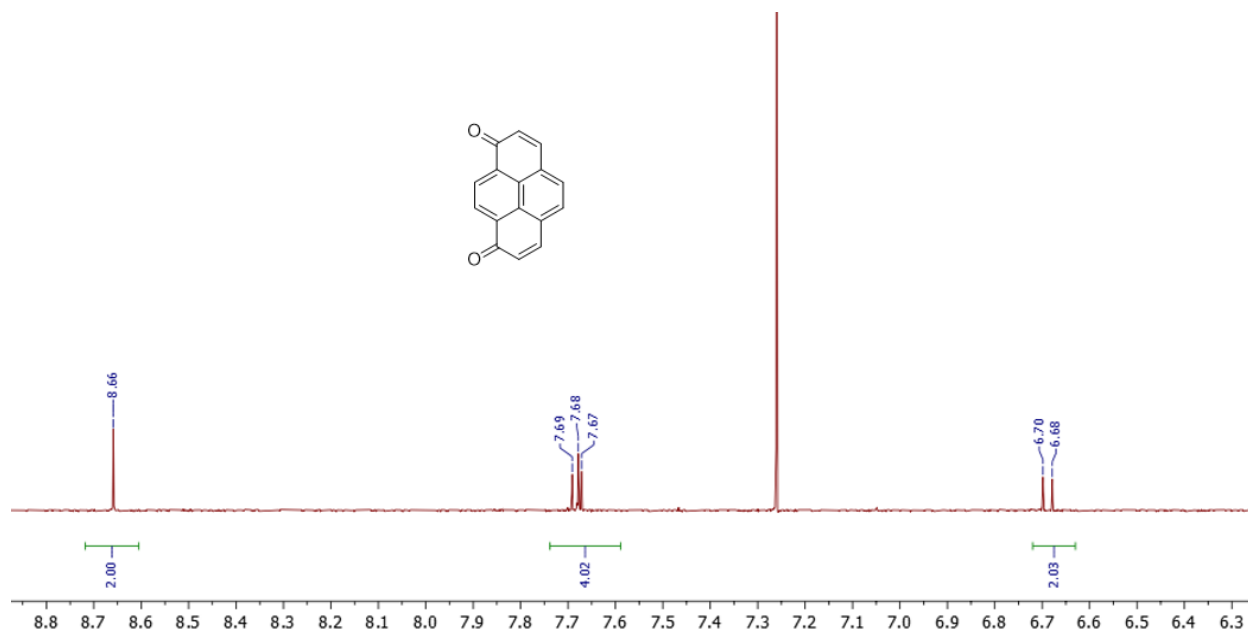


Fig. S13. ^1H NMR in CDCl_3 at 500 MHz of **6a** isolated as minor product from the **1a**-IBX reaction. The downfield alkene doublet overlaps with an aromatic singlet at 7.68.

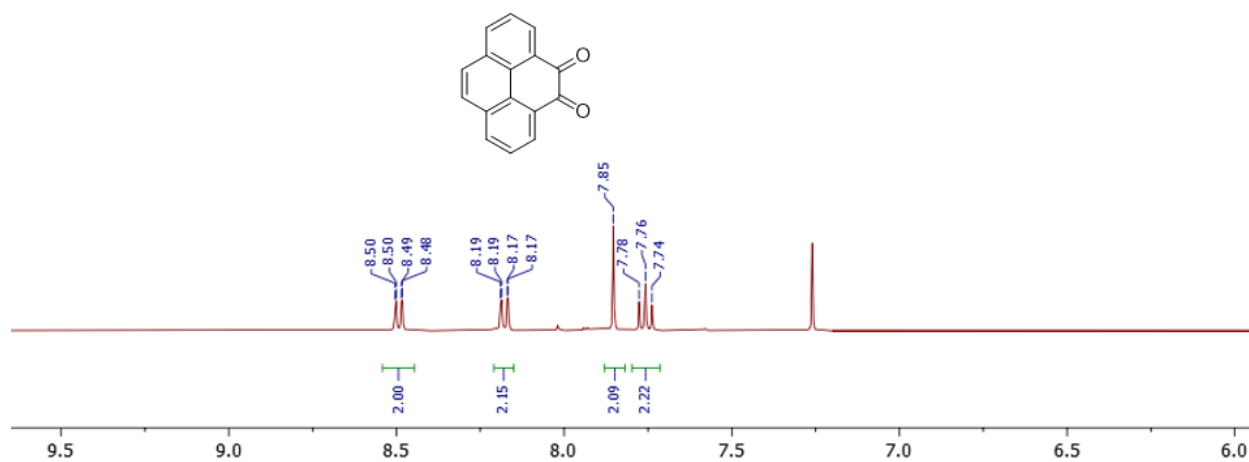


Fig. S14. ^1H NMR in CDCl_3 at 400 MHz of **2a** isolated as minor product from the **1a**-IBX reaction.

1b- H_5IO_6 reaction

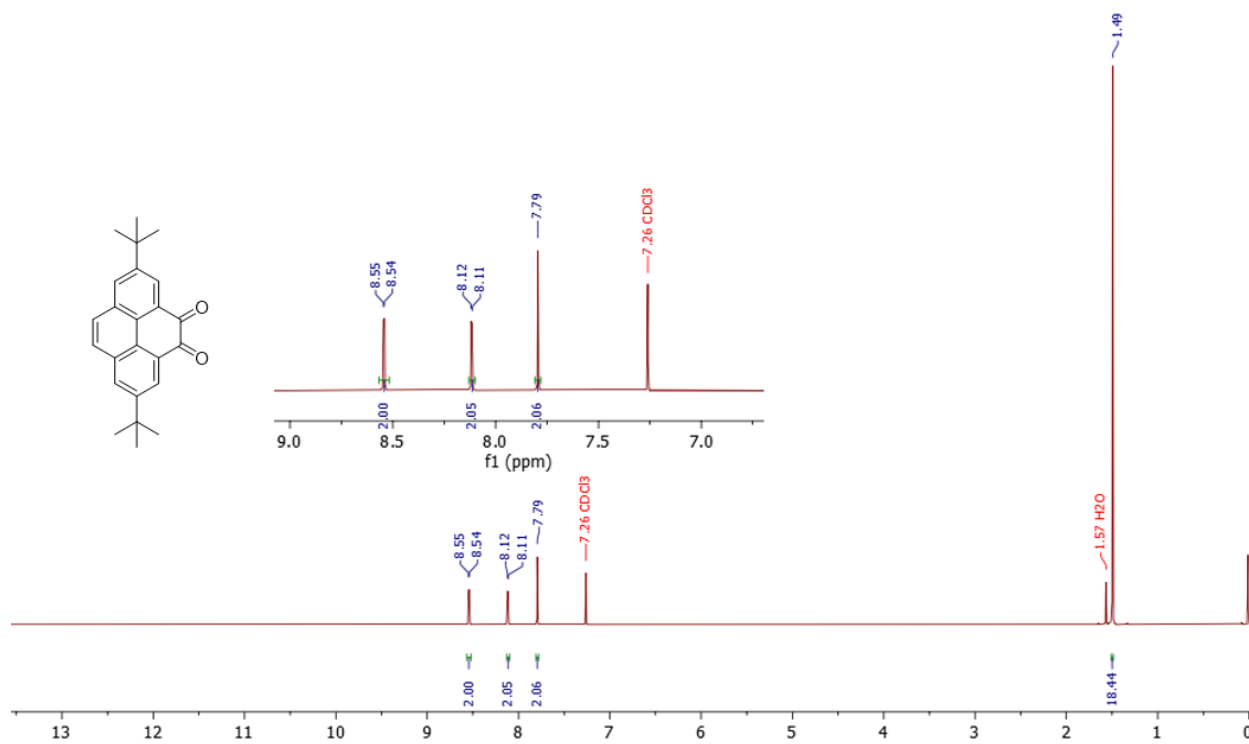


Fig. S15. ^1H NMR in CDCl_3 at 400 MHz of crude **2b** (after the vacuum filtration step) isolated as single product from the **1b**- H_5IO_6 reaction.

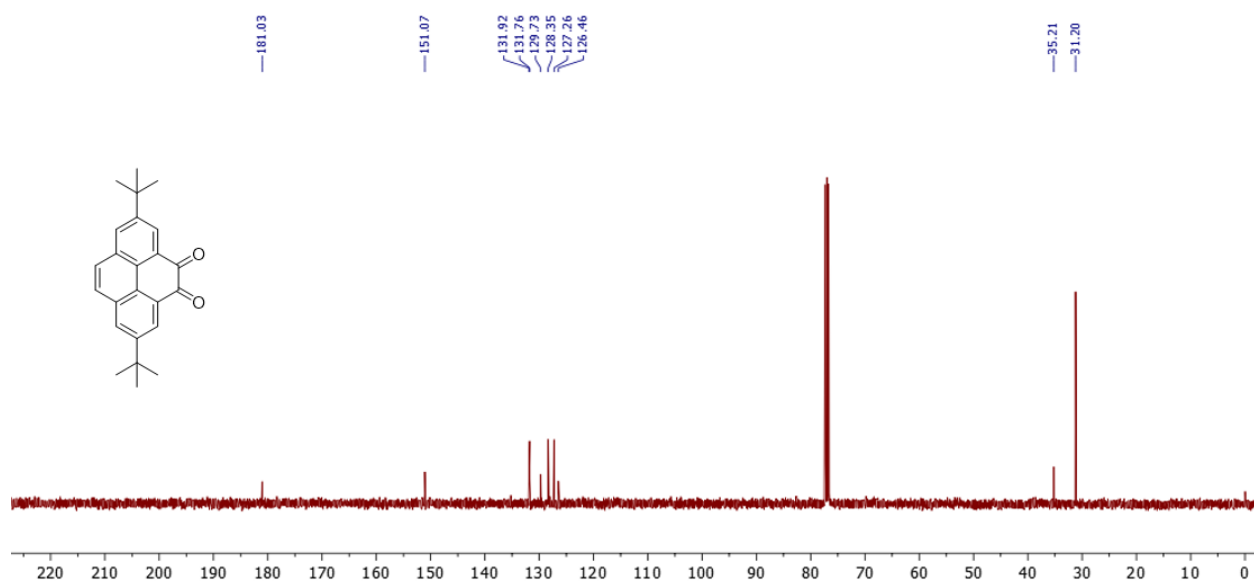


Fig. S16. ¹³C NMR in CDCl₃ at 100 MHz of **2b** isolated as single product from the **1b**- H₅IO₆ reaction.

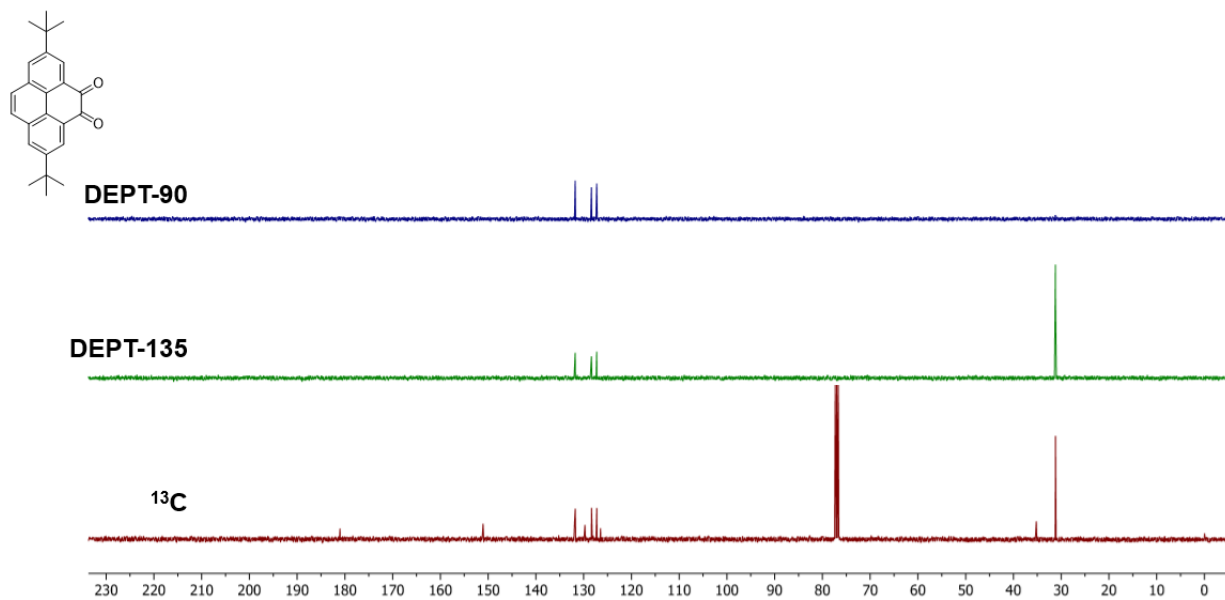


Fig. S17. ¹³C NMR of **2b** in CDCl₃ at 100 MHz (red), DEPT-135 (green) and DEPT-90 (blue).

1b-HIO₃ reaction

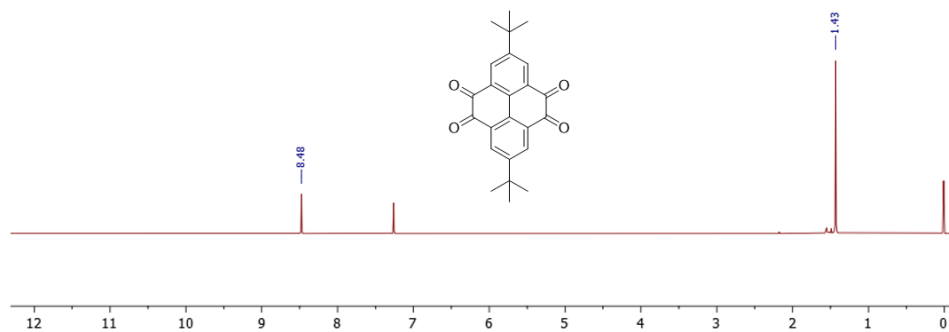


Fig. S18. ¹H NMR in CDCl₃ at 400 MHz of crude **3b** (after the vacuum filtration step) isolated as single product from the **1b**-HIO₃ reaction.

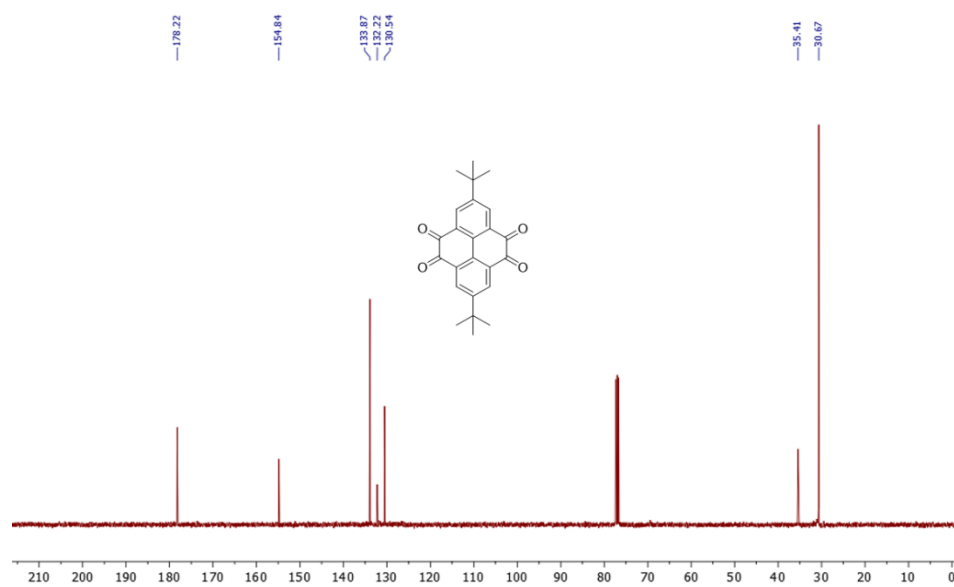


Fig. S19. ¹³C NMR in CDCl₃ at 100 MHz of **3b** isolated as single product from the **1b**-HIO₃ reaction.

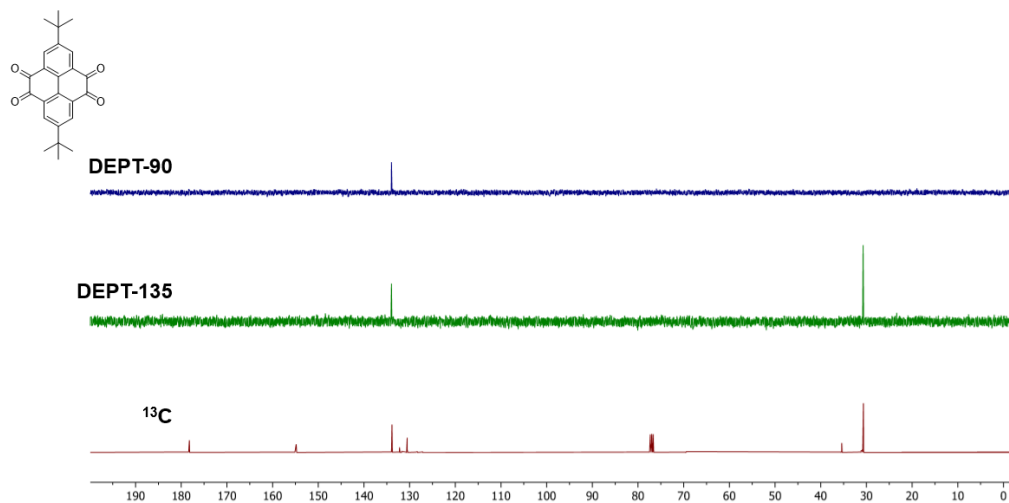


Fig. S20. ¹³C NMR of **3b** in CDCl₃ at 100 MHz (red), DEPT-135 (green) and DEPT-90 (blue).

1b-IBX reaction

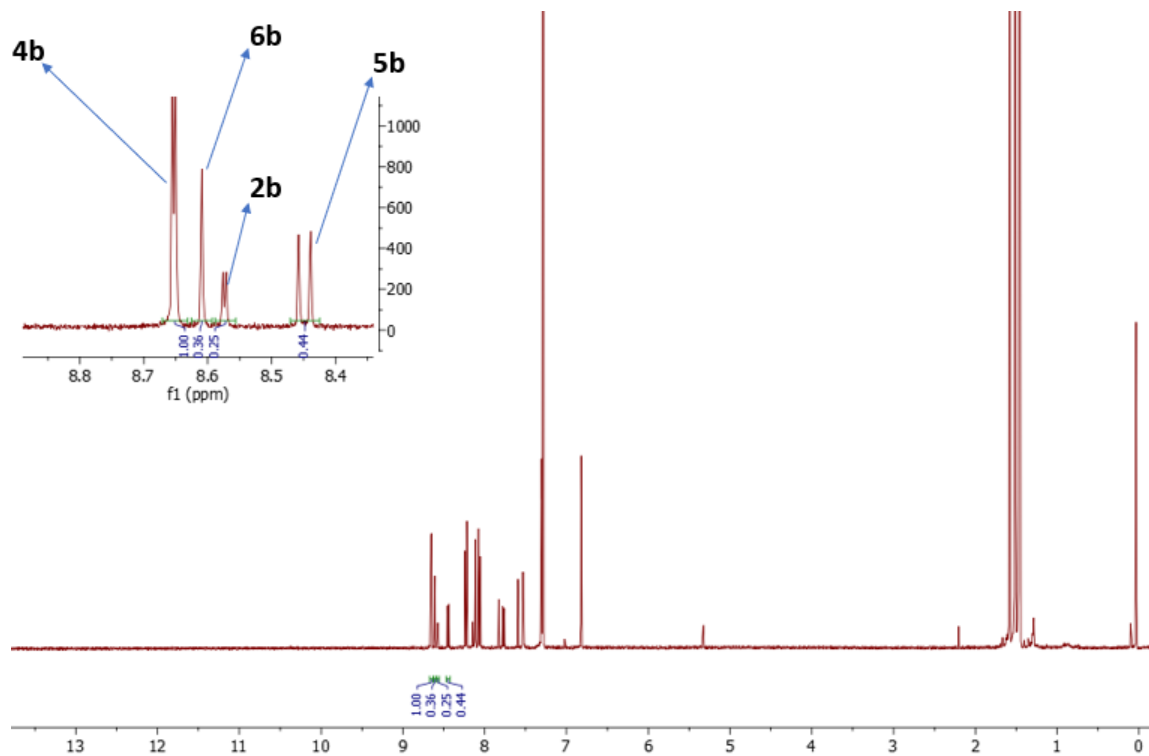


Fig. S21. ¹H NMR in CDCl₃ at 400 MHz of the crude product from the **1b**-IBX reaction.

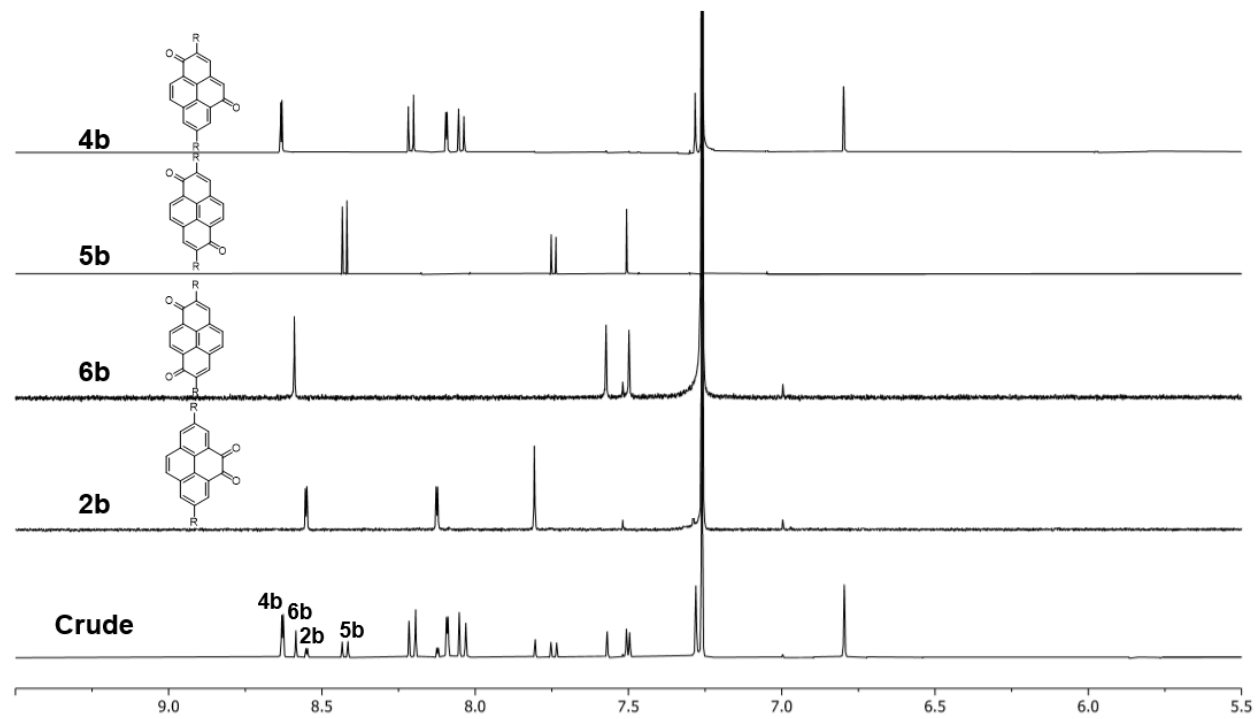


Fig. S22. ¹H NMR spectra of all isolated diones from the **1b**-IBX reaction vs. the crude (decreasing yield from top downwards), R=*tert*-butyl.

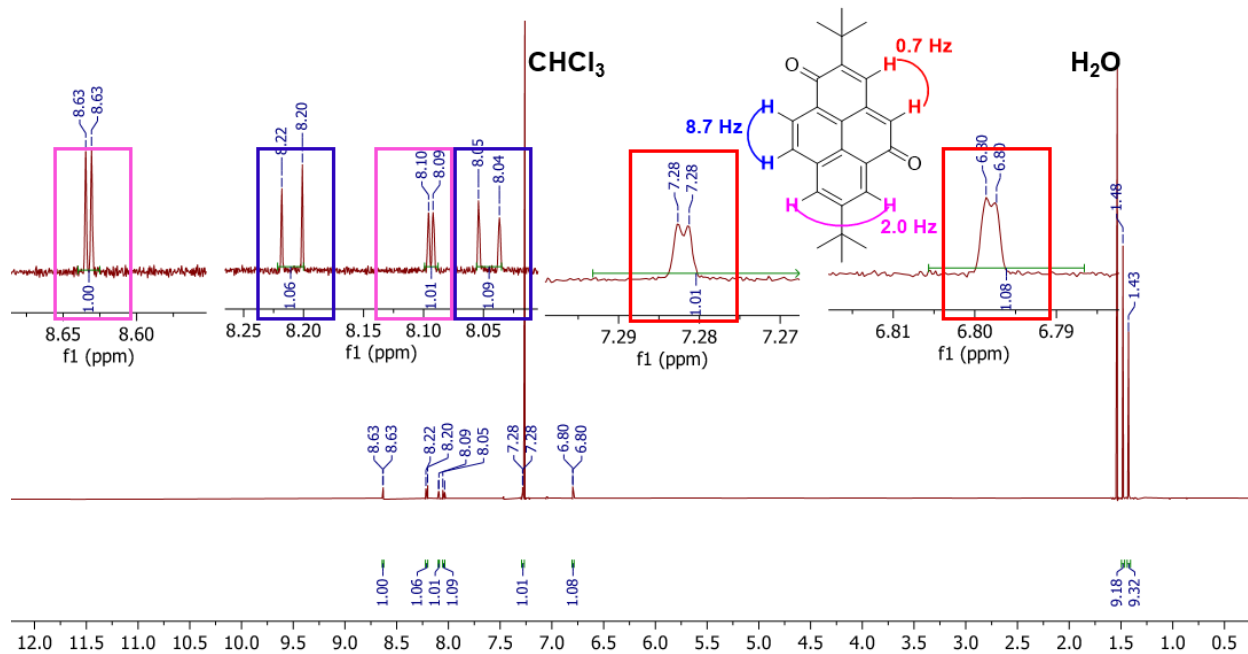


Fig. S23. ^1H NMR in CDCl_3 at 500 MHz of **4b** isolated as major product from the **1b**-IBX reaction.

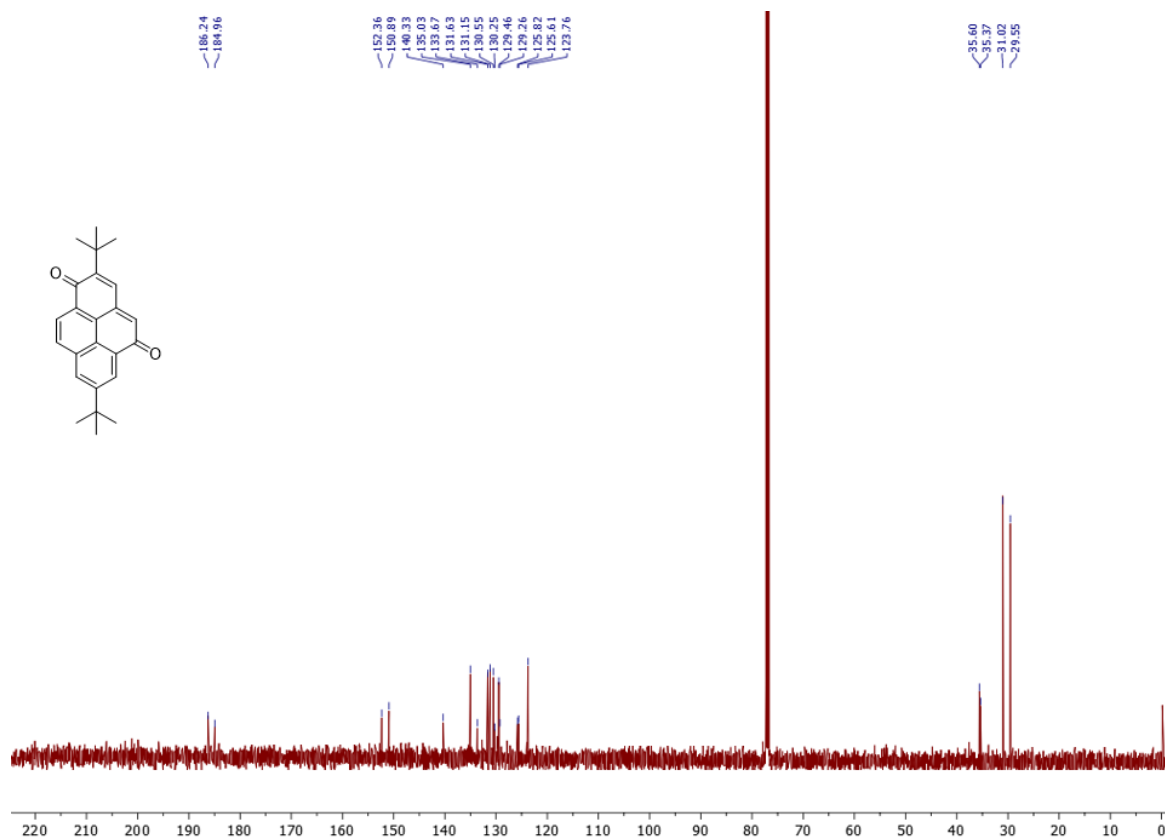


Fig. S24. ^{13}C NMR in CDCl_3 at 125 MHz of **4b** isolated as major product from the **1b**-IBX reaction.

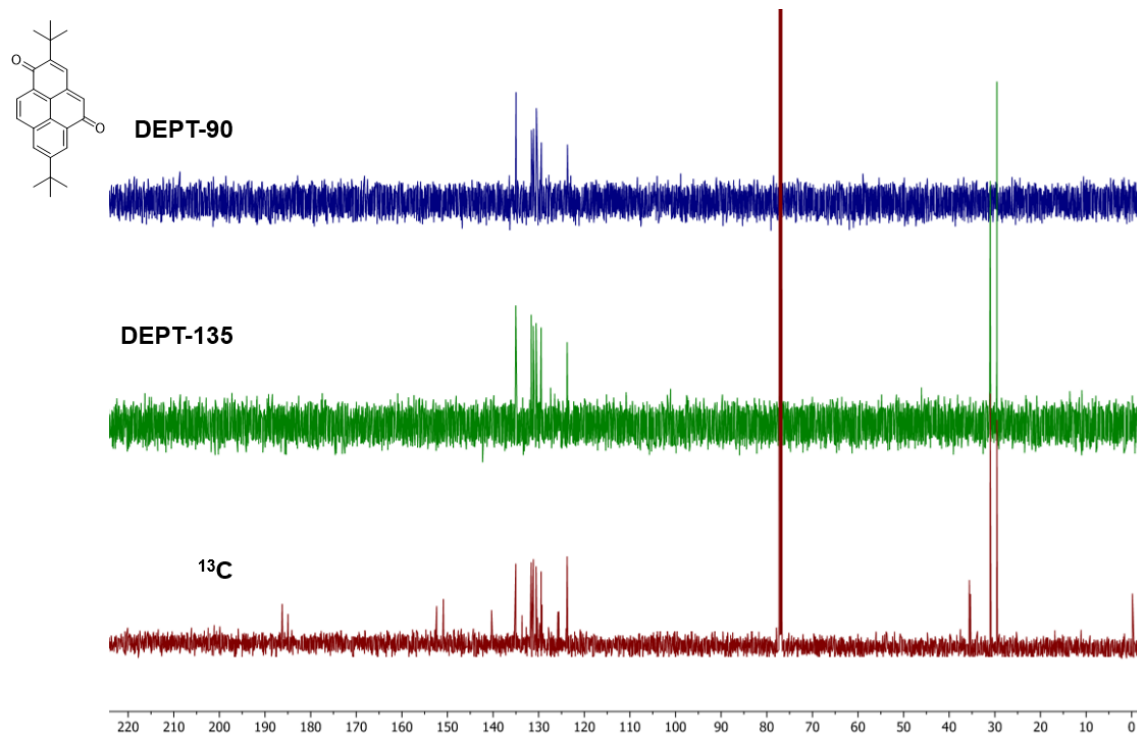


Fig. S25. ^{13}C NMR of **4b** in CDCl_3 at 125 MHz (red), DEPT-135 (green) and DEPT-90 (blue).

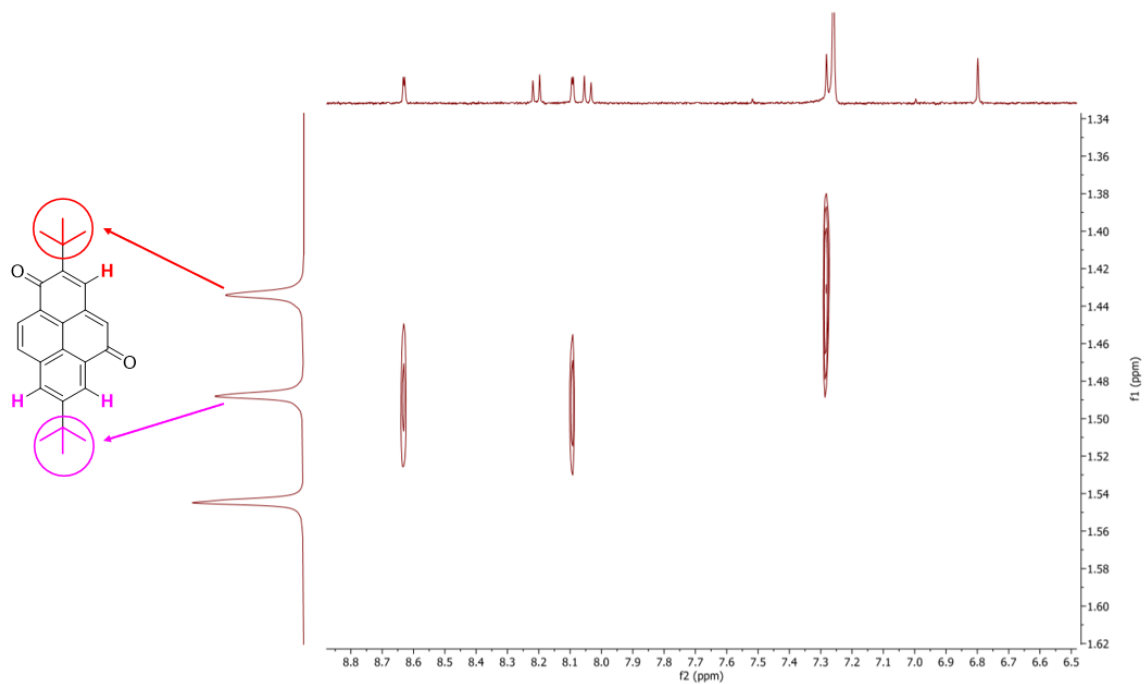


Fig. S26. 2D- $(^1\text{H}$ - ^1H , ROESY) NMR for aliphatic (vertical) vs. aromatic (horizontal) protons of **4b**.

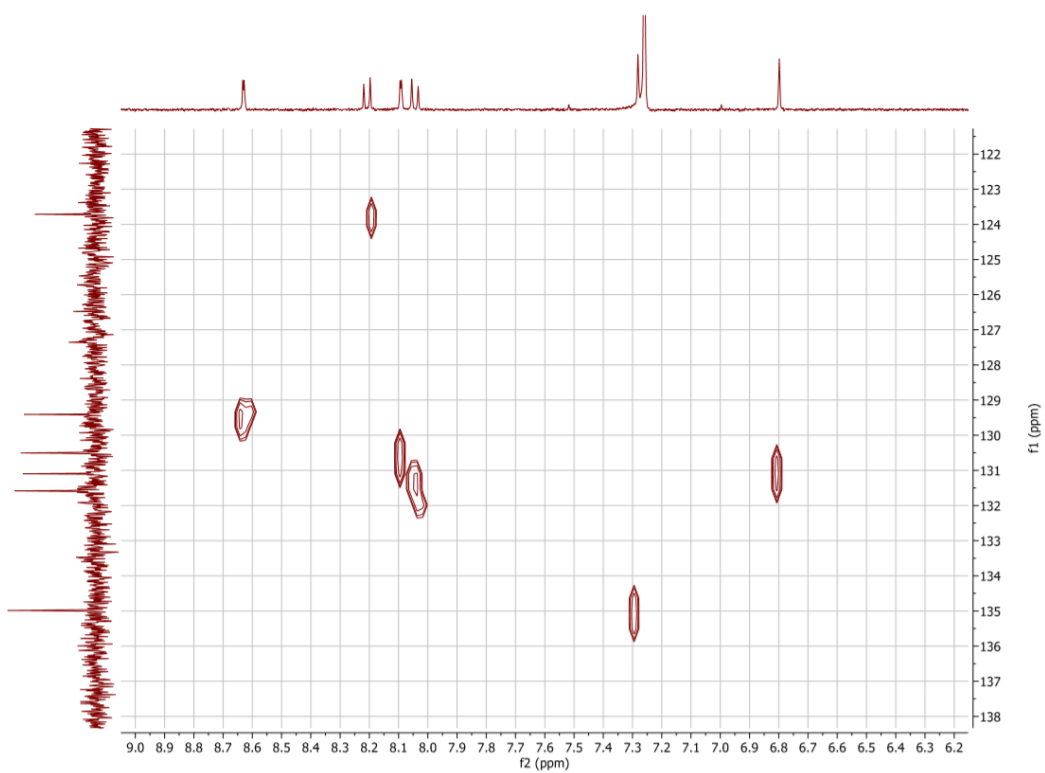


Fig. S27. 2D-(¹H-¹³C, HSQC) NMR for aromatic carbons (vertical) vs. aromatic protons (horizontal) of **4b**.

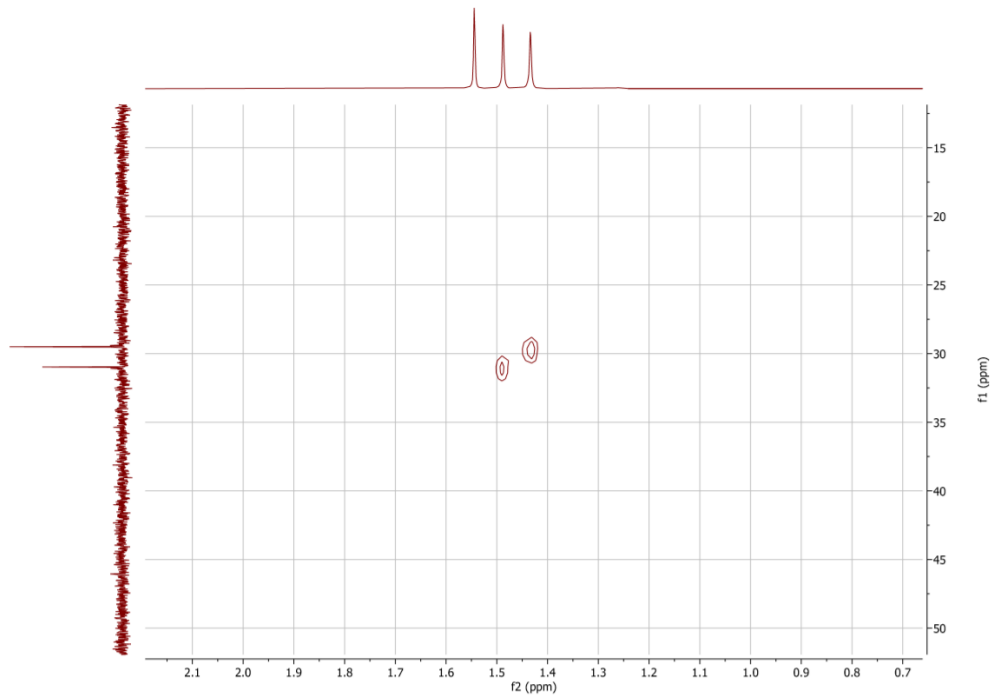


Fig. S28. 2D-(¹H-¹³C, HSQC) NMR for aliphatic carbons (vertical) vs. aliphatic protons (horizontal) of **4b**.

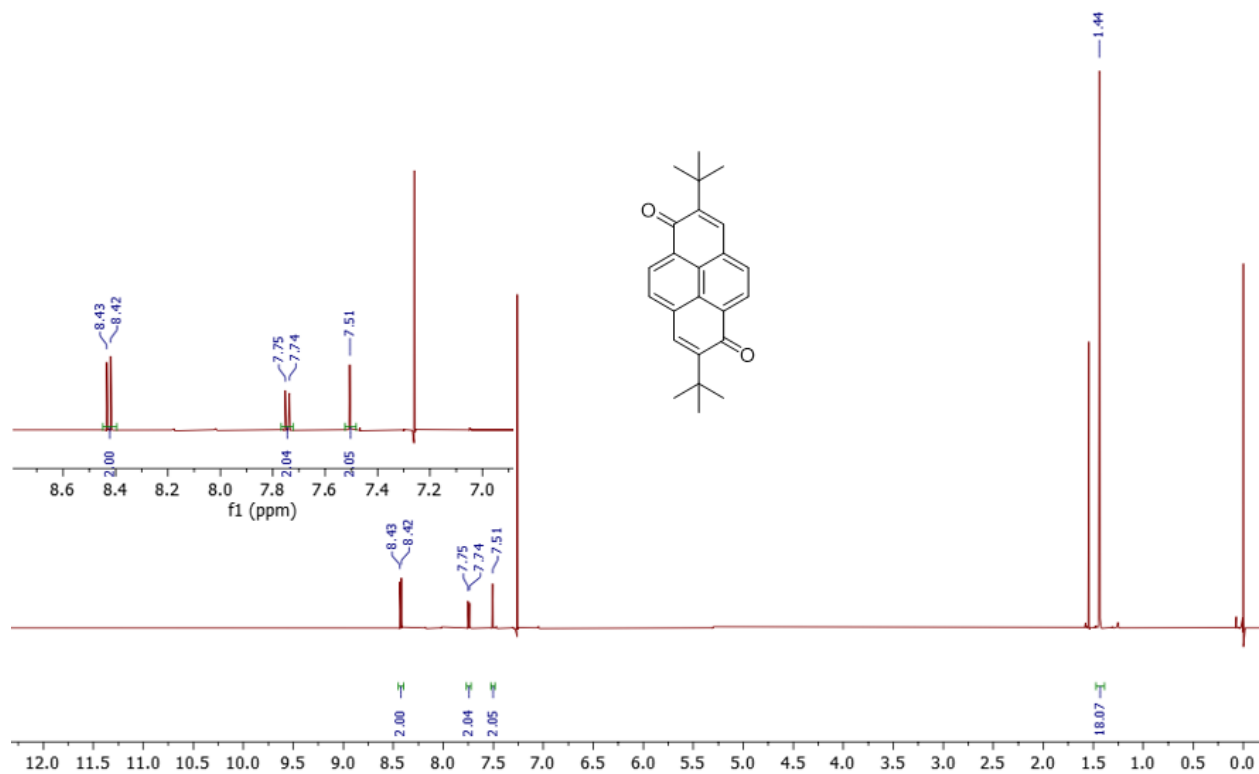


Fig. S29. ¹H NMR in CDCl₃ at 500 MHz of **5b** isolated as minor product from the **1b**-IBX reaction.

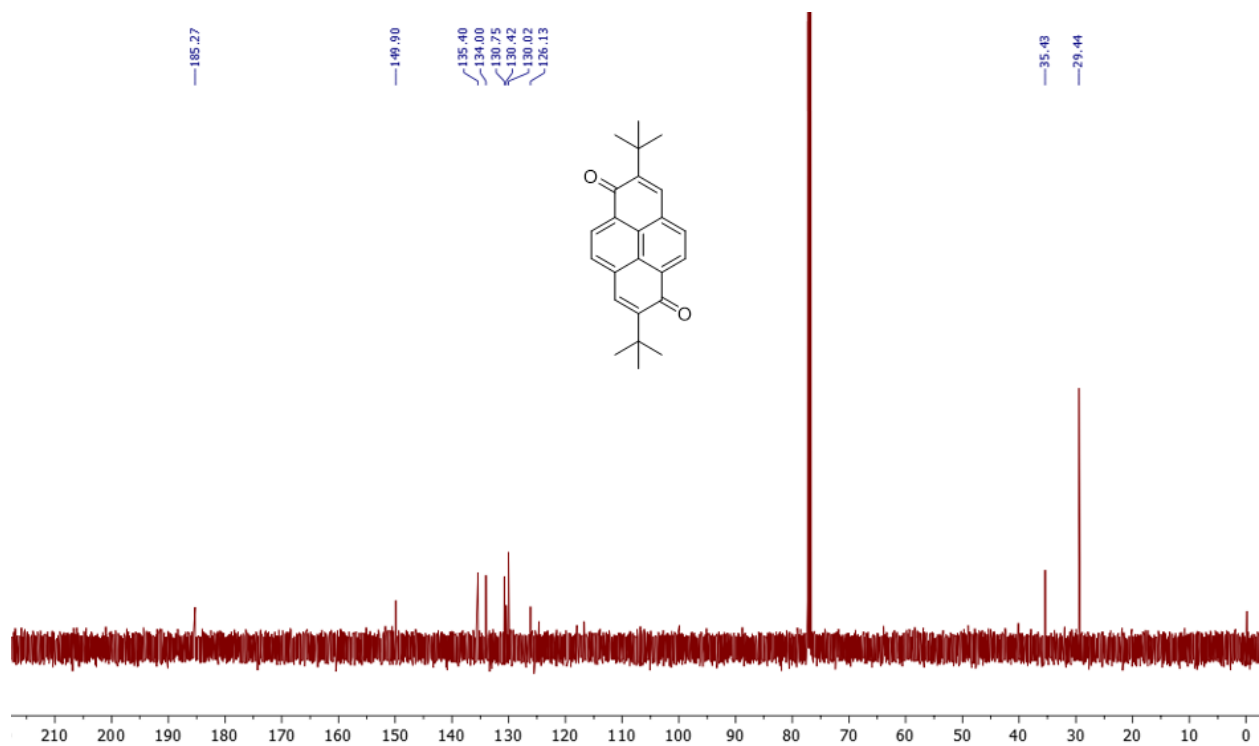


Fig. S30. ¹³C NMR in CDCl₃ at 125 MHz of **5b** isolated as minor product from the **1b**-IBX reaction.

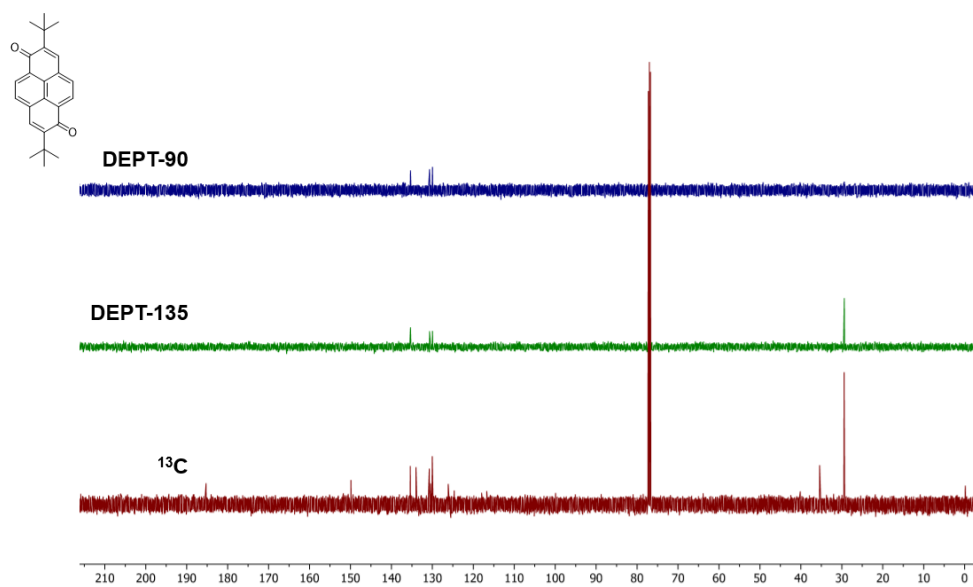


Fig. S31. ¹³C NMR of **5b** in CDCl₃ at 125 MHz (red), DEPT-135 (green) and DEPT-90 (blue).

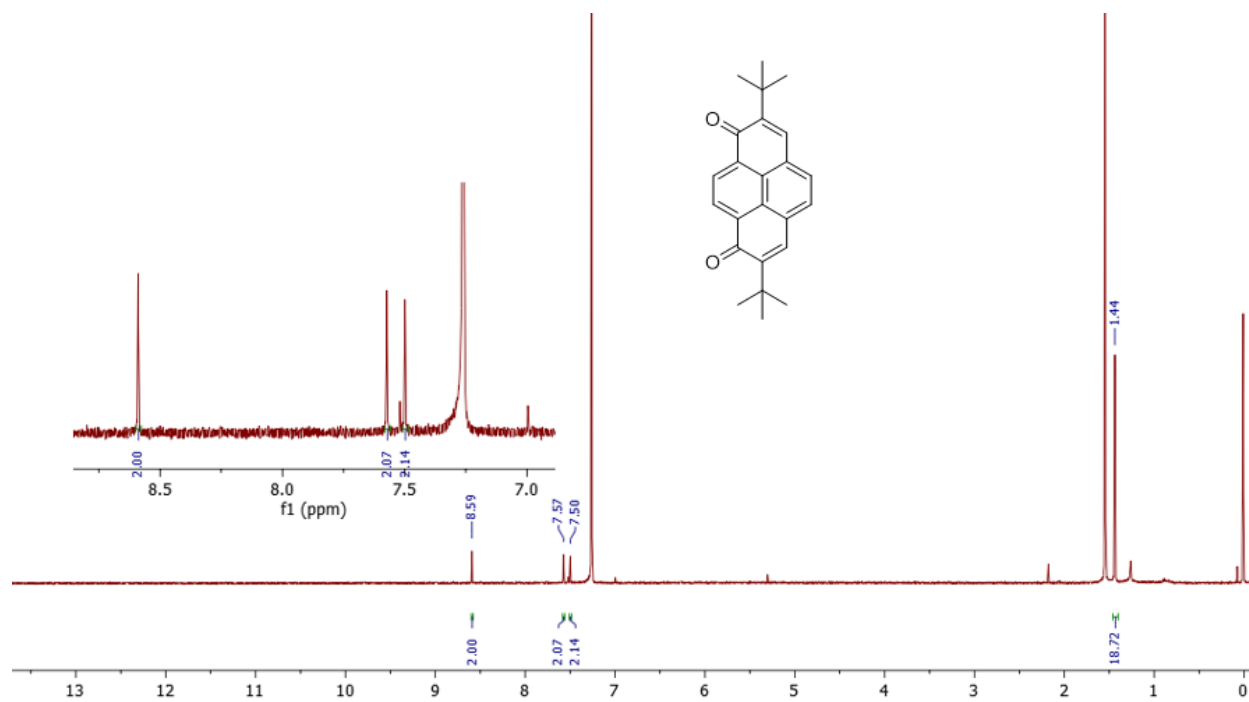


Fig. S32. ¹H NMR in CDCl₃ at 400 MHz of **6b** isolated as minor product from the **1b**-IBX reaction.

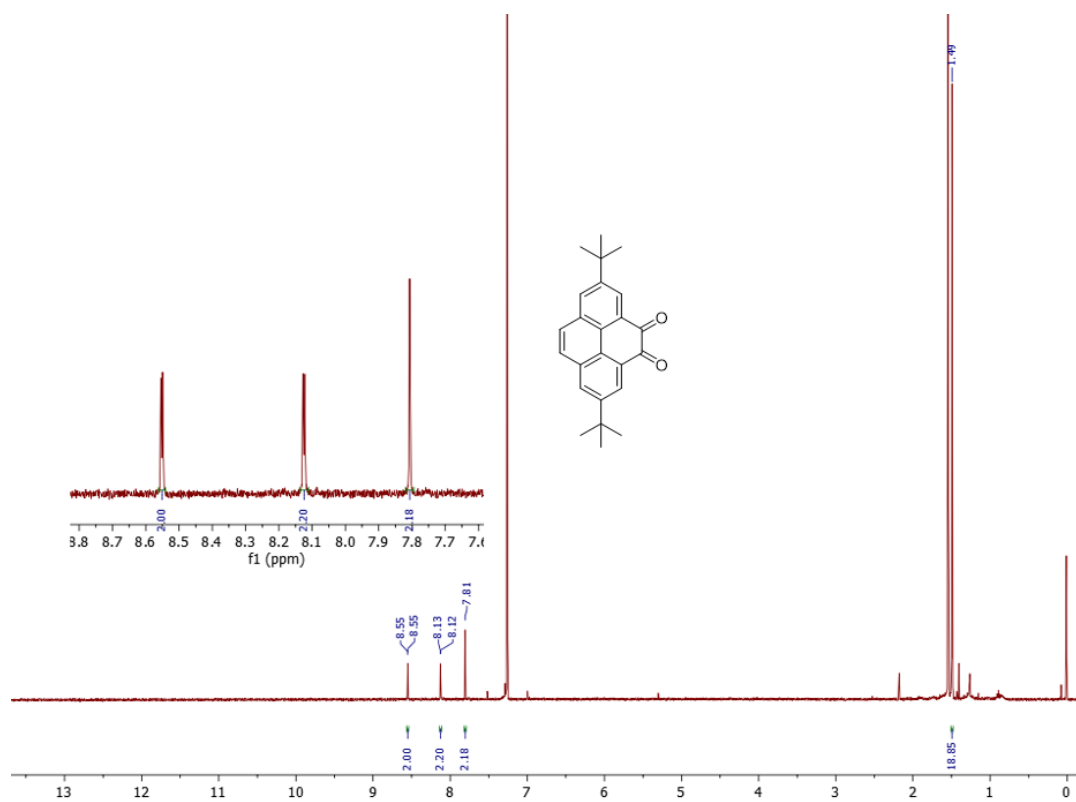


Fig. S33. ^1H NMR in CDCl_3 at 400 MHz of **2b** isolated as minor product from the **1b**-IBX reaction.

Other reactions:

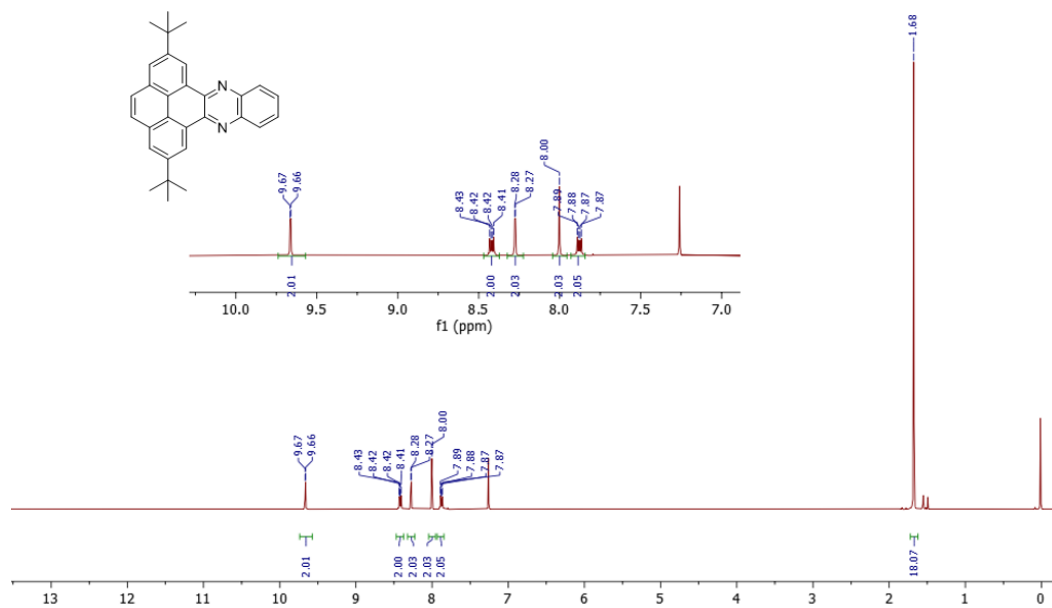


Fig. S34. ^1H NMR in CDCl_3 at 400 MHz of **8** synthesized directly from **1b** through crude **2b**.

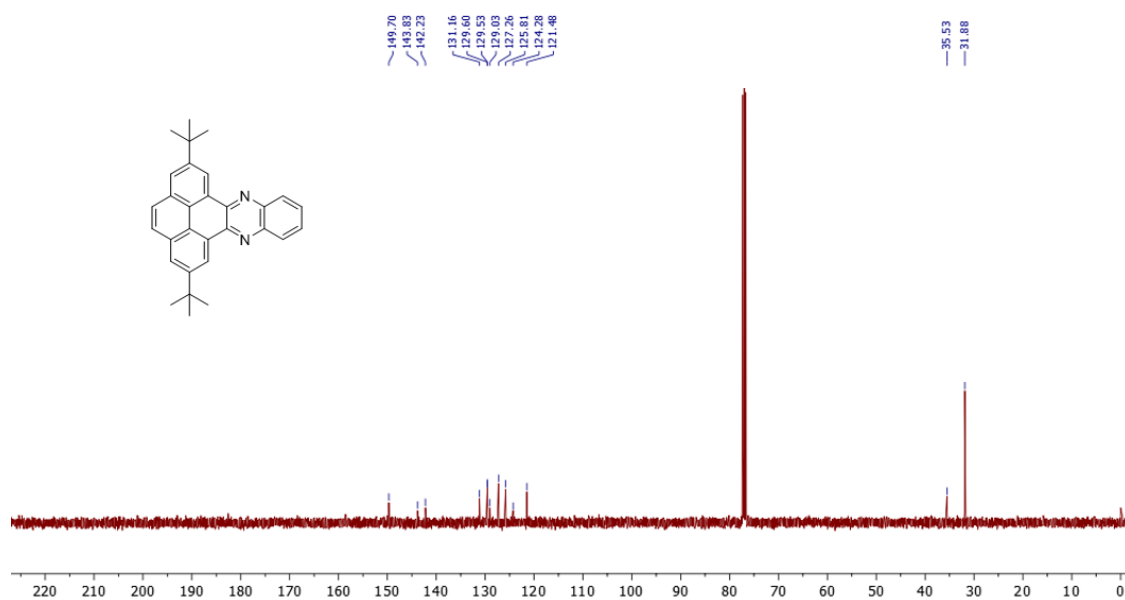


Fig. S35. ¹³C NMR in CDCl₃ at 100 MHz of **8** synthesized directly from **1b** through crude **2b**.

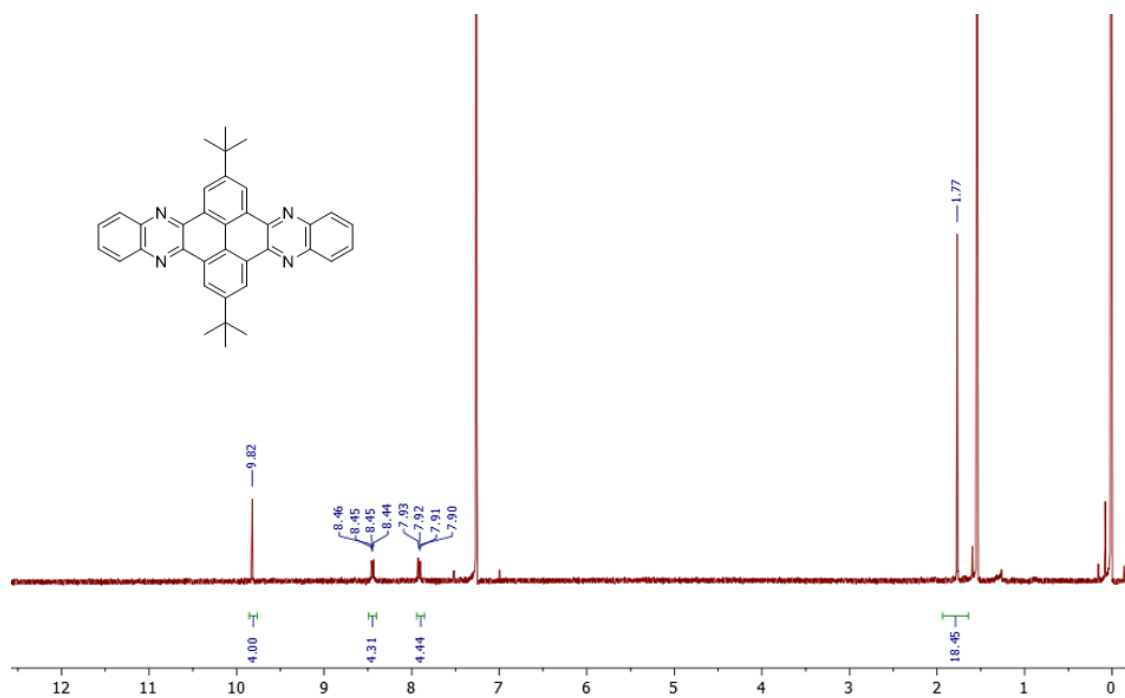


Fig. S36. ¹H NMR in CDCl₃ at 400 MHz of **9** synthesized directly from **1b** through crude **3b**.

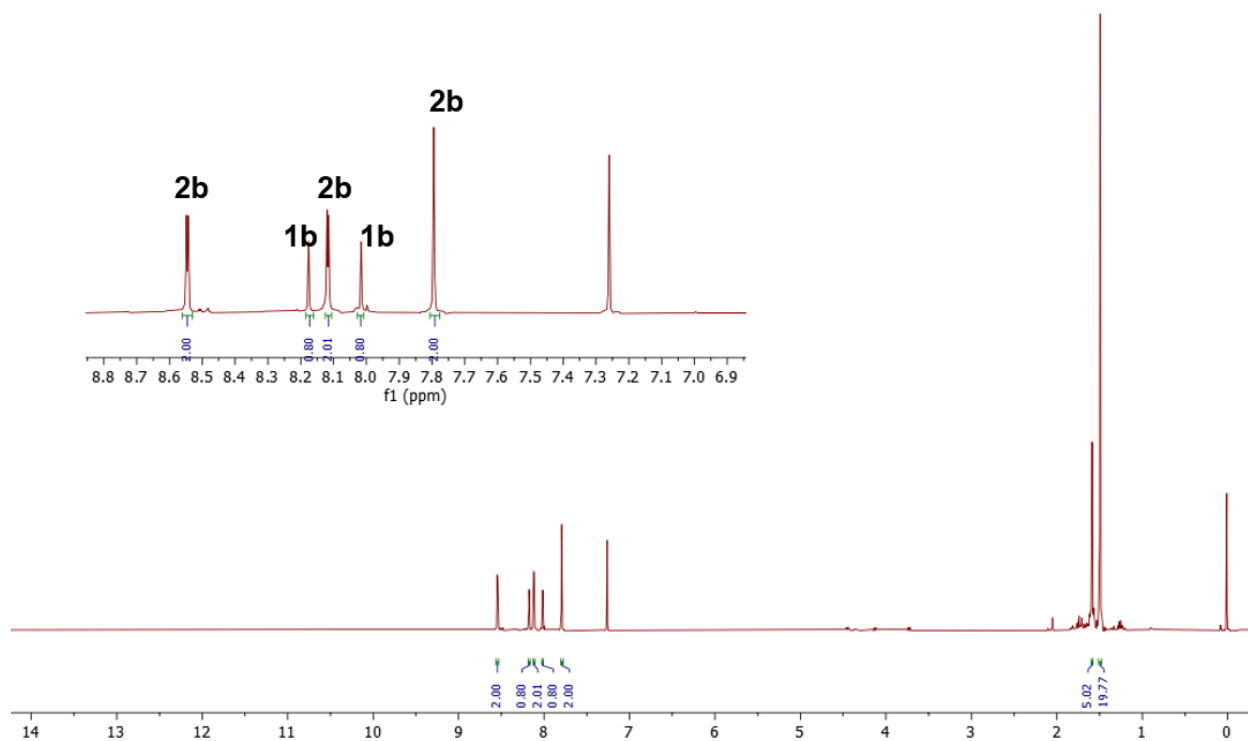


Fig. S37. ¹H NMR in CDCl₃ at 400 MHz of the crude product isolated from our very first **1b** iodination attempt using I₂/HIO₃ in AcOH at reflux (**2b** and unreacted **1b** with almost no impurity).

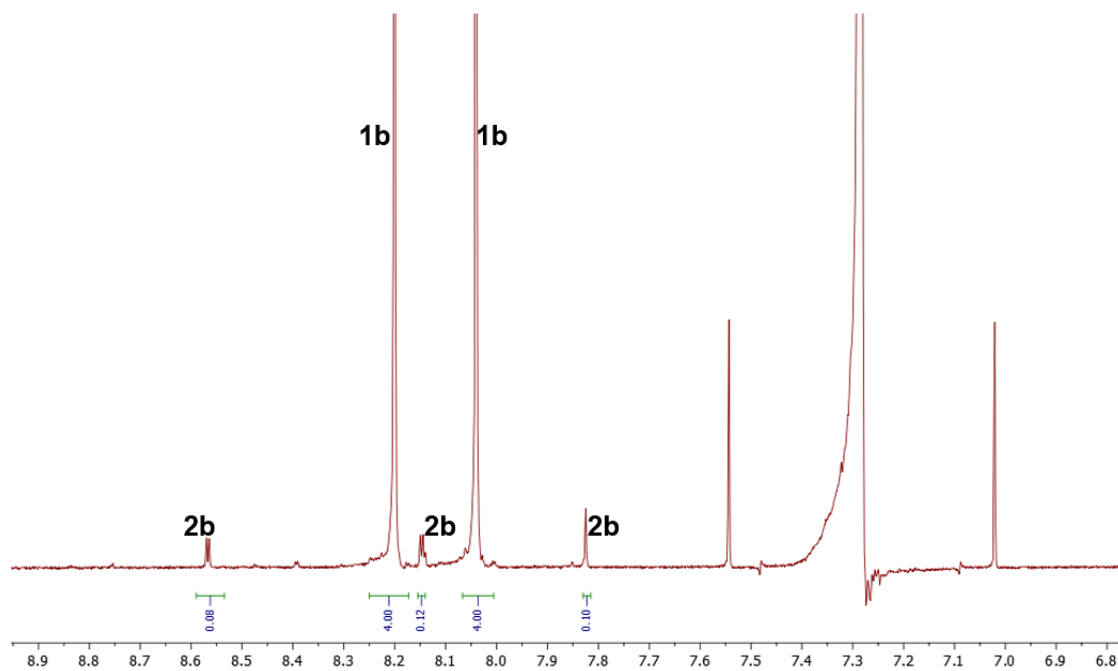


Fig. S38. ¹H NMR in CDCl₃ at 400 MHz of the crude product isolated from oxidation of **1b** using with 4 mol equivalents of NaIO₄ in AcOH after 16 h at reflux.

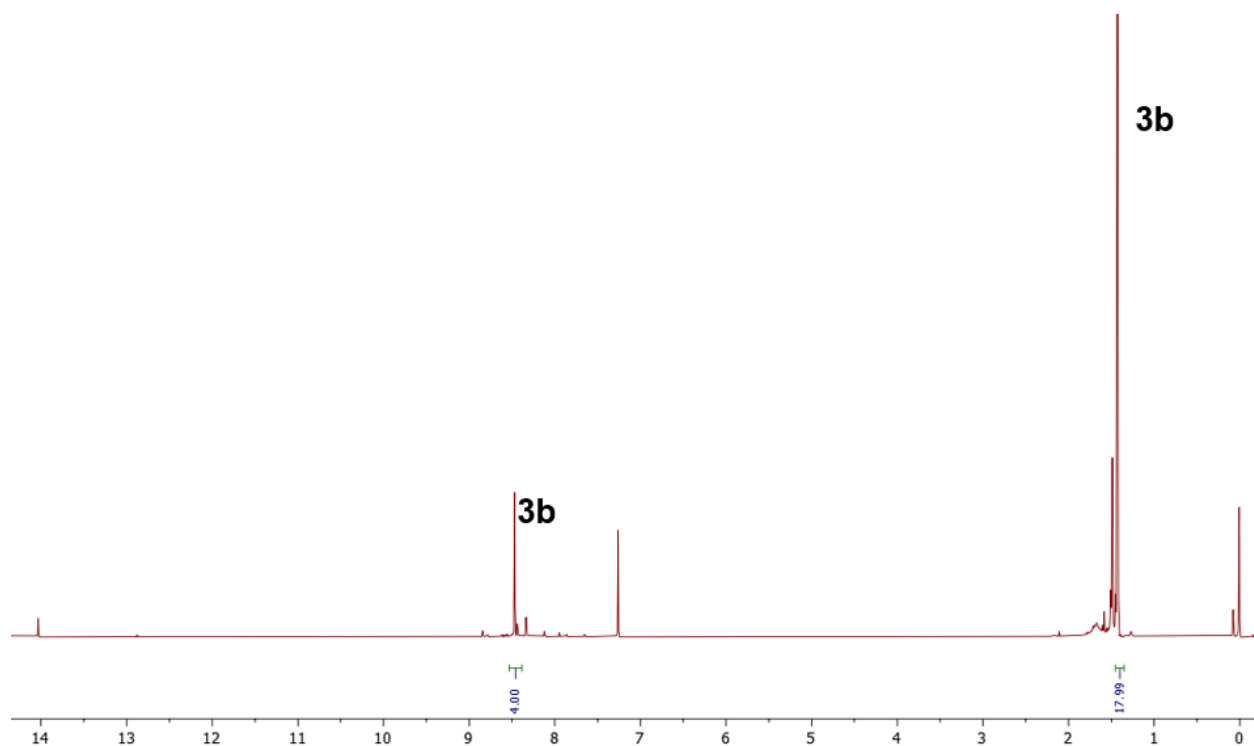


Fig. S39. ^1H NMR in CDCl_3 at 400 MHz of the crude product isolated from the oxidation of **1b** with 4 mol equivalents of NaIO_4 in AcOH with H_2SO_4 after reflux for 3 h (H_2SO_4 drives the oxidation forward in AcOH).

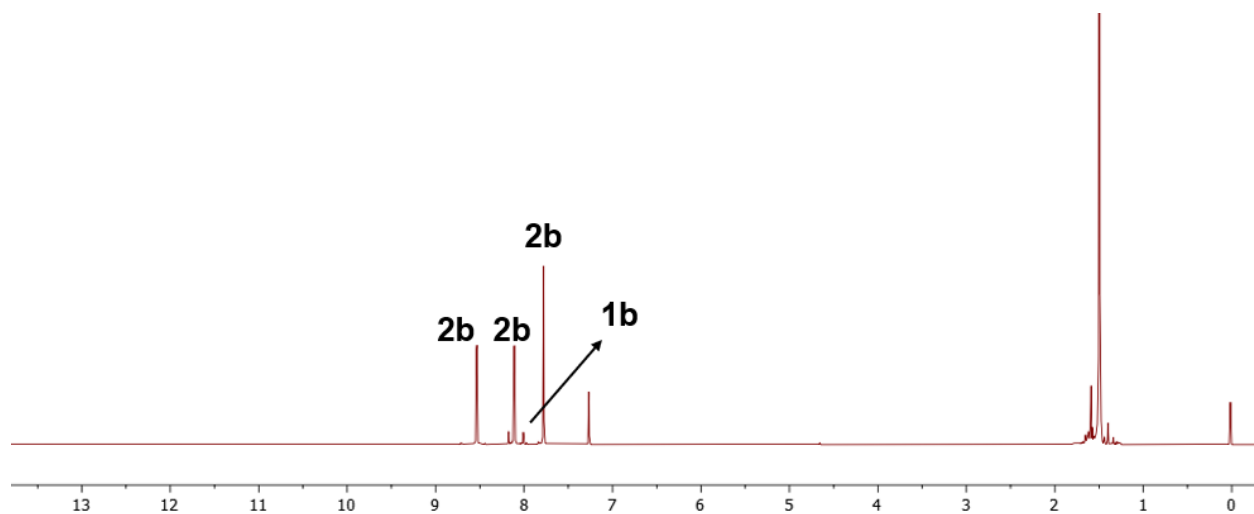


Fig. S40. ^1H NMR in CDCl_3 at 400 MHz of the crude product isolated from **1b** oxidation with 4 mol equivalents of H_5IO_6 in EtOH on 10 g scale after 5 h at reflux (with some unreacted **1b**).

VIII. UV-Vis, HRMS, IR Data:

UV-Vis absorption spectra:

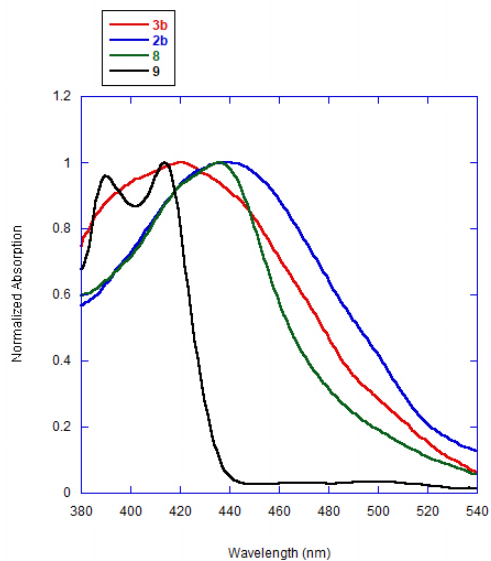


Fig. S41. Normalized absorption spectra of **2b** and **3b**, and their corresponding *N*-heteroacenes **8** and **9**. **2b/3b/8** in EtOH, **9** in DCM.

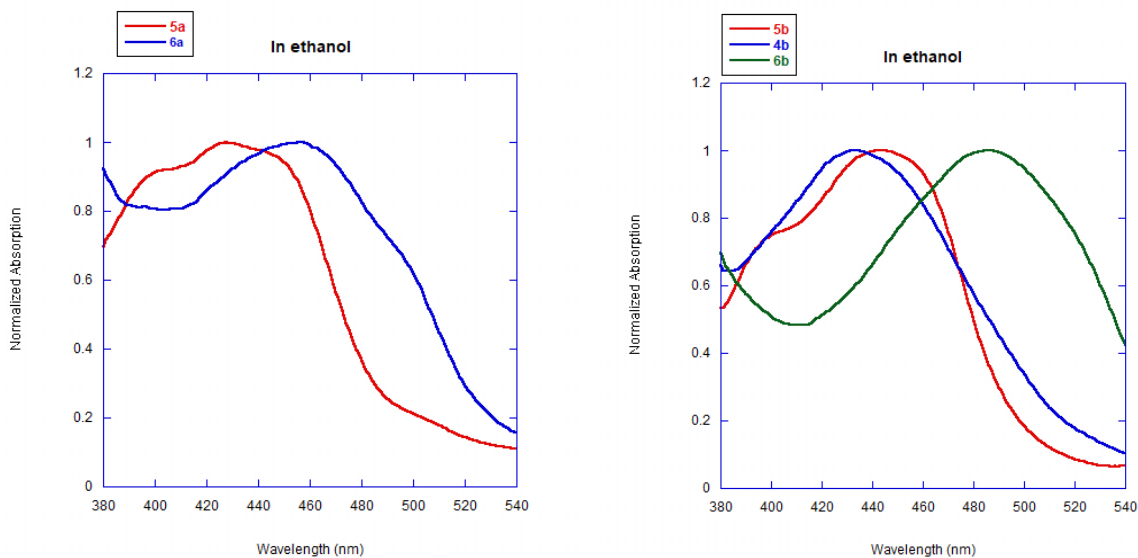


Fig. S42. Normalized absorption spectra of **4b**, **5a/5b** and **6a/6b** in EtOH.

High resolution mass spectrometry:

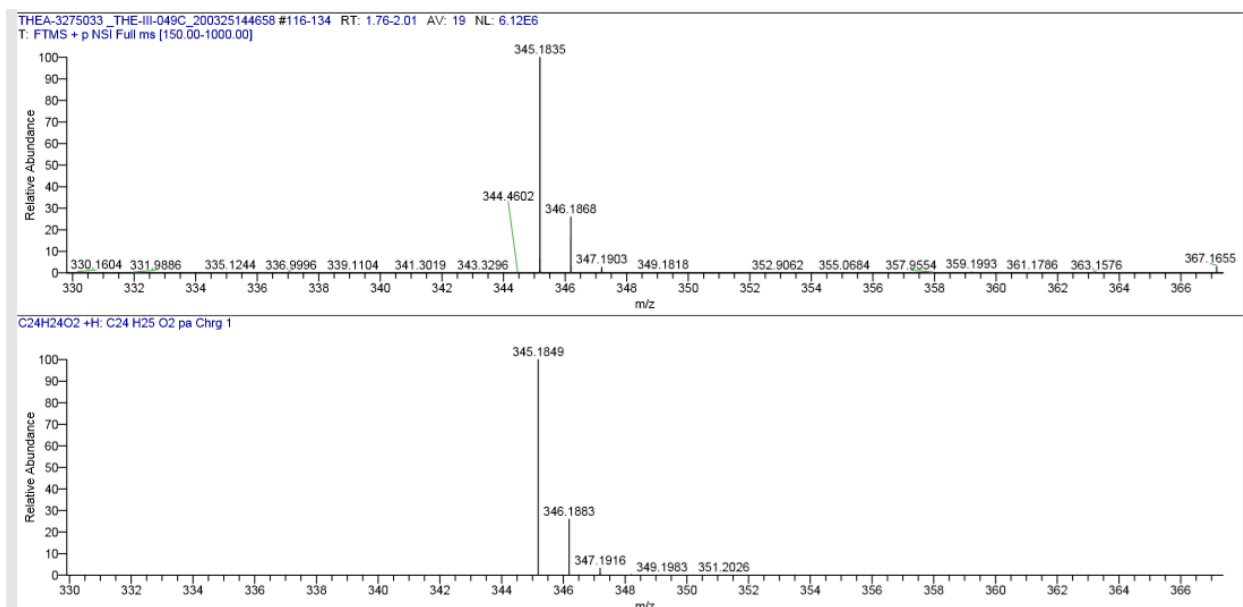


Fig. S43. HRMS (ESI/Orbitrap) of **2b** (top) vs. theoretical $[M+H]^+$ (bottom).

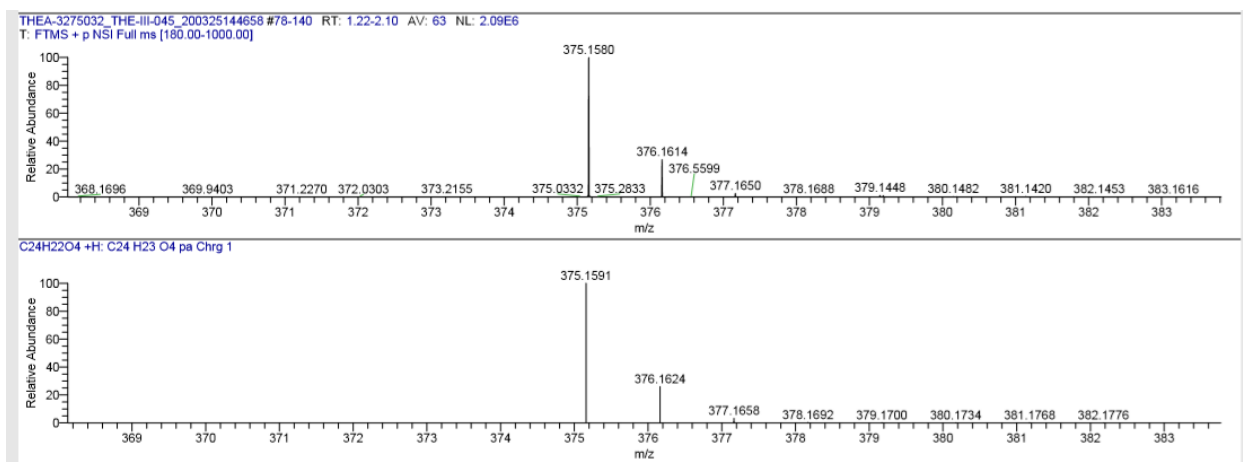


Fig. S44. HRMS (ESI/Orbitrap) of **3b** (top) vs. theoretical $[M+H]^+$ (bottom).

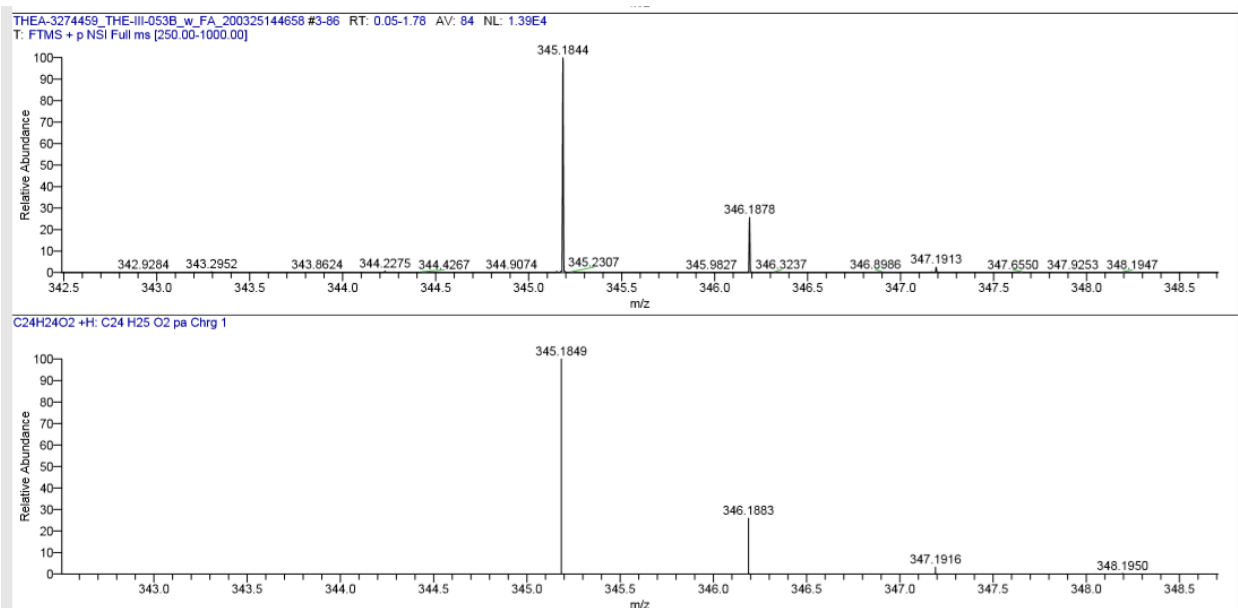


Fig. S45. HRMS (ESI/Orbitrap) of **4b** (top) vs. theoretical $[M+H]^+$ (bottom).

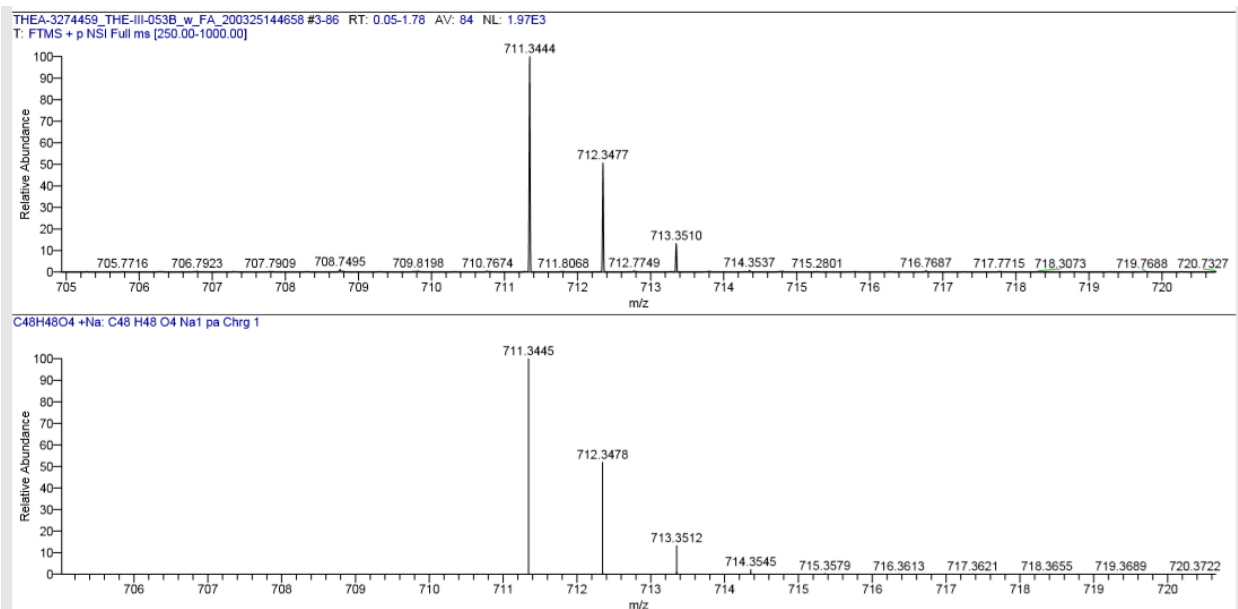


Fig. S46. HRMS (ESI/Orbitrap) of **4b** (top) vs. theoretical $[2M+Na]^+$ (bottom).

FT-IR spectra of the purified compounds in KBr:

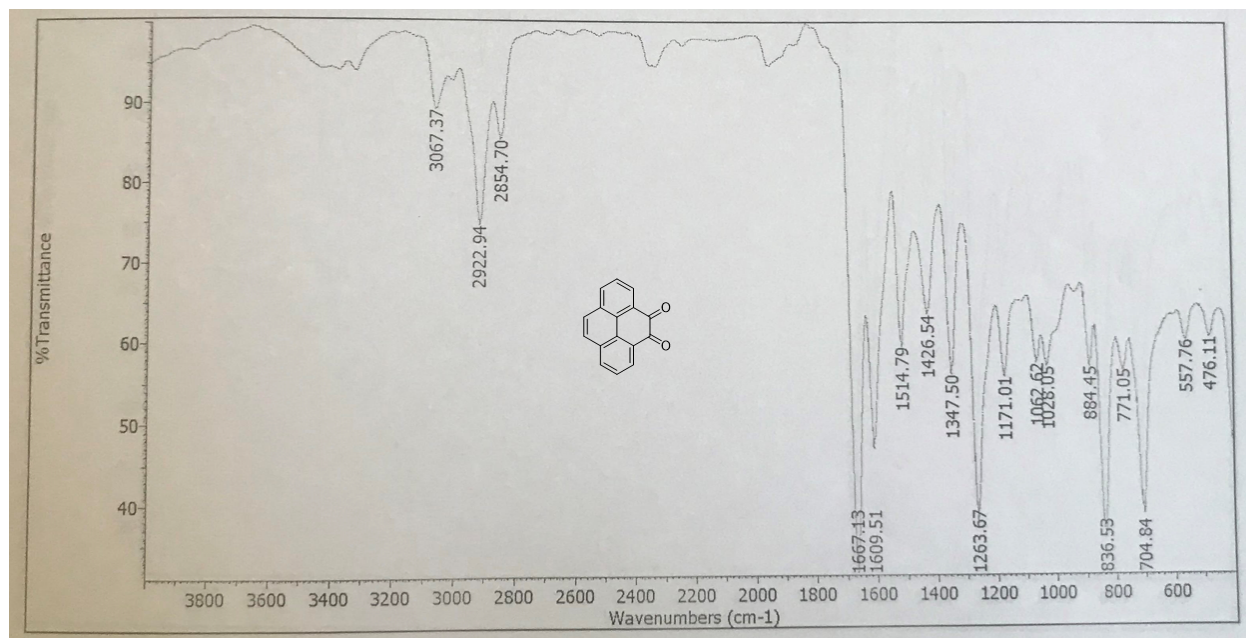


Fig. S47. FT-IR (KBr) of 2a.

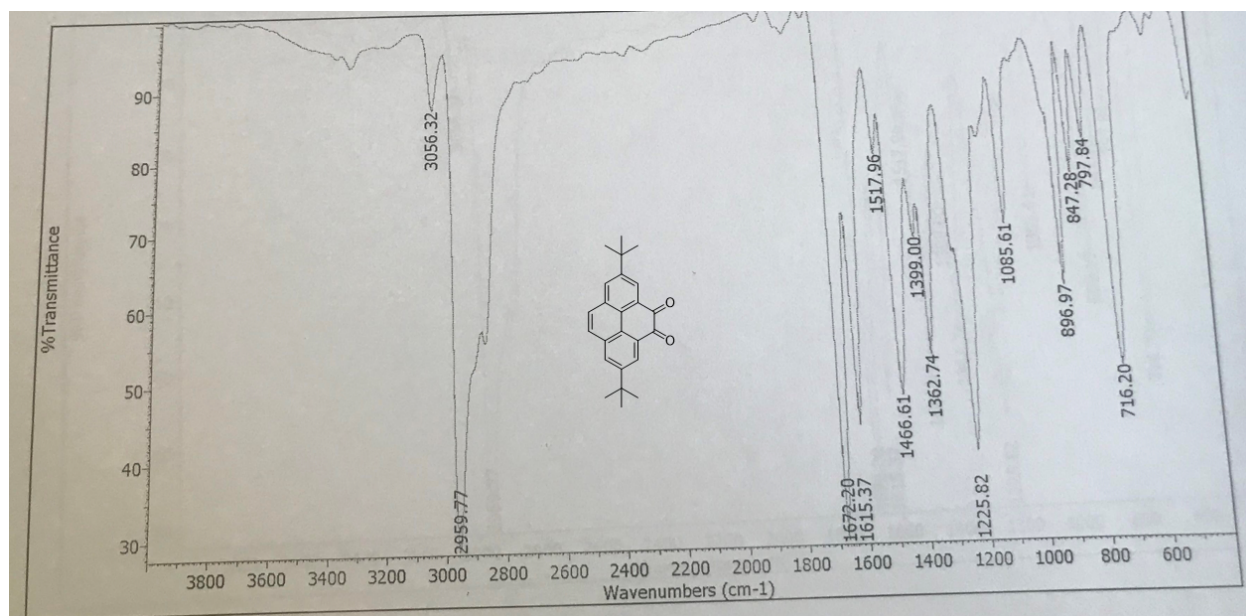


Fig. S48. FT-IR (KBr) of 2b.

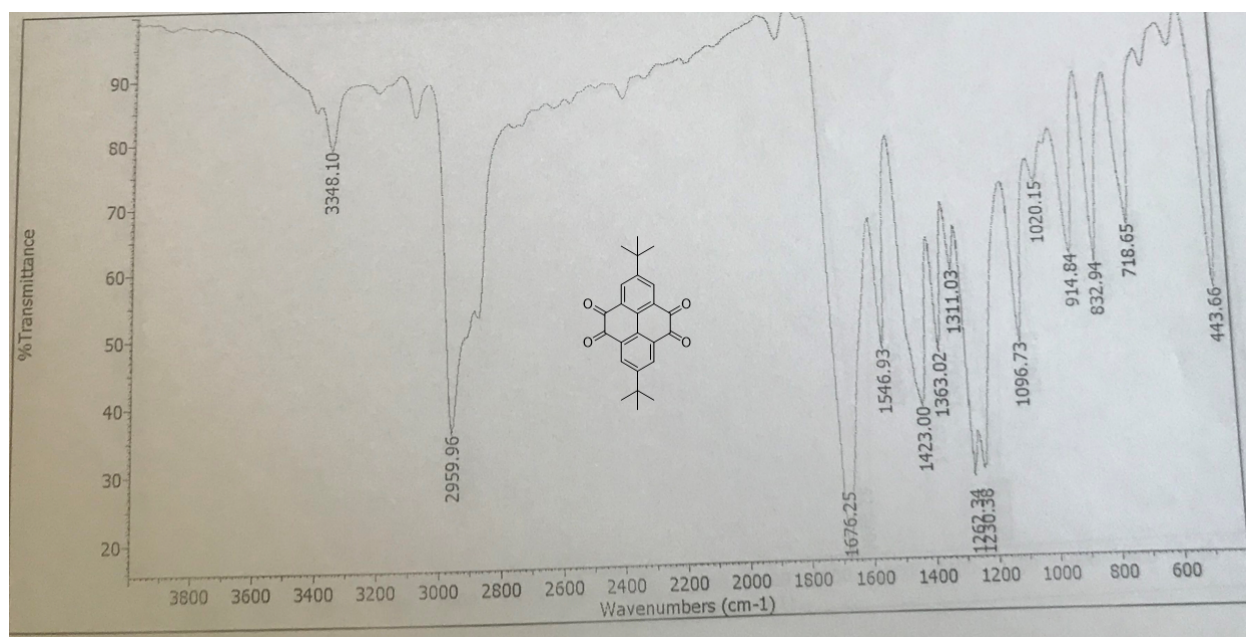


Fig. S49. FT-IR (KBr) of 3b.

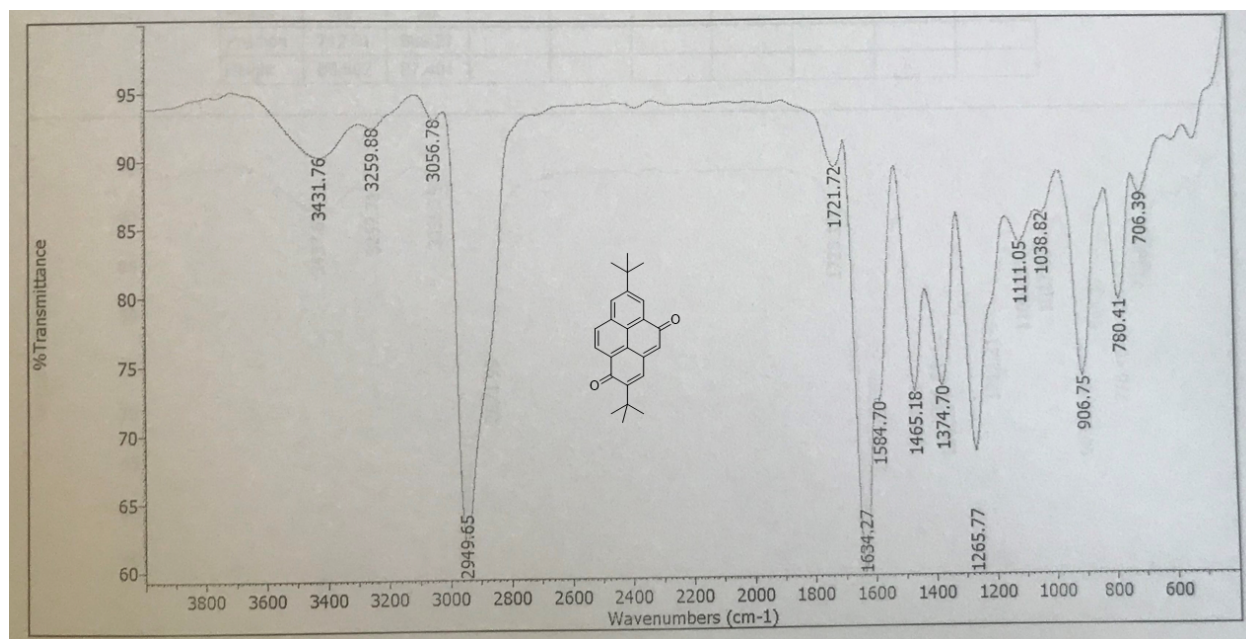


Fig. S50. FT-IR (KBr) of 4b.

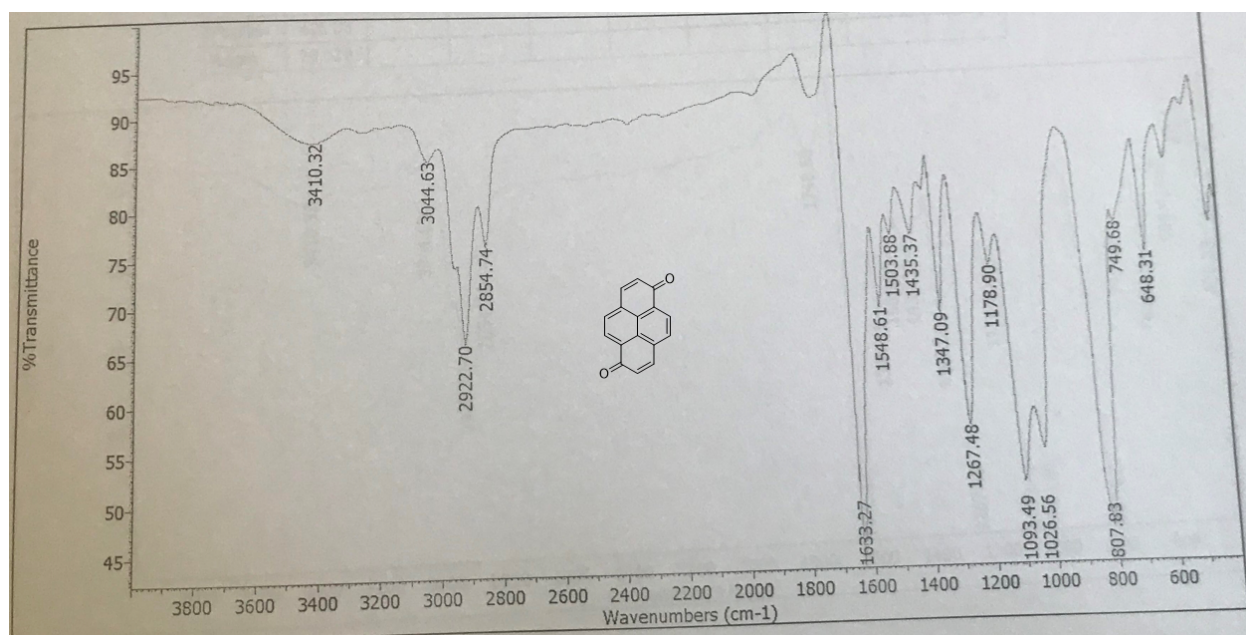


Fig. S51. FT-IR (KBr) of 5a.

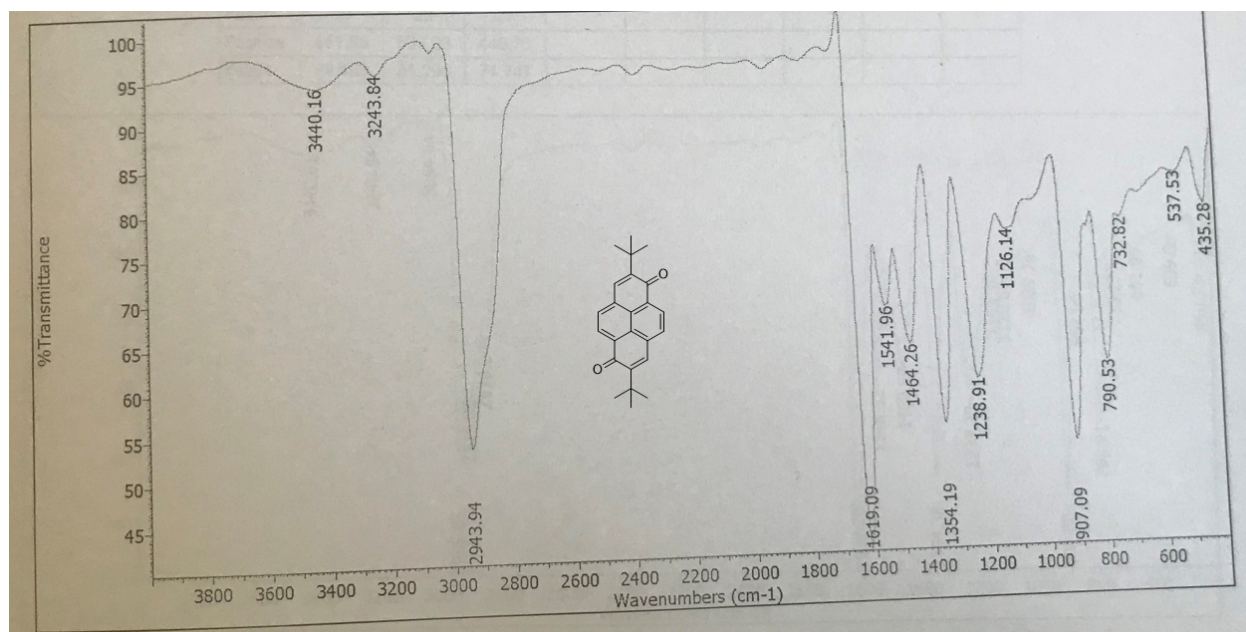


Fig. S52. FT-IR (KBr) of 5b.

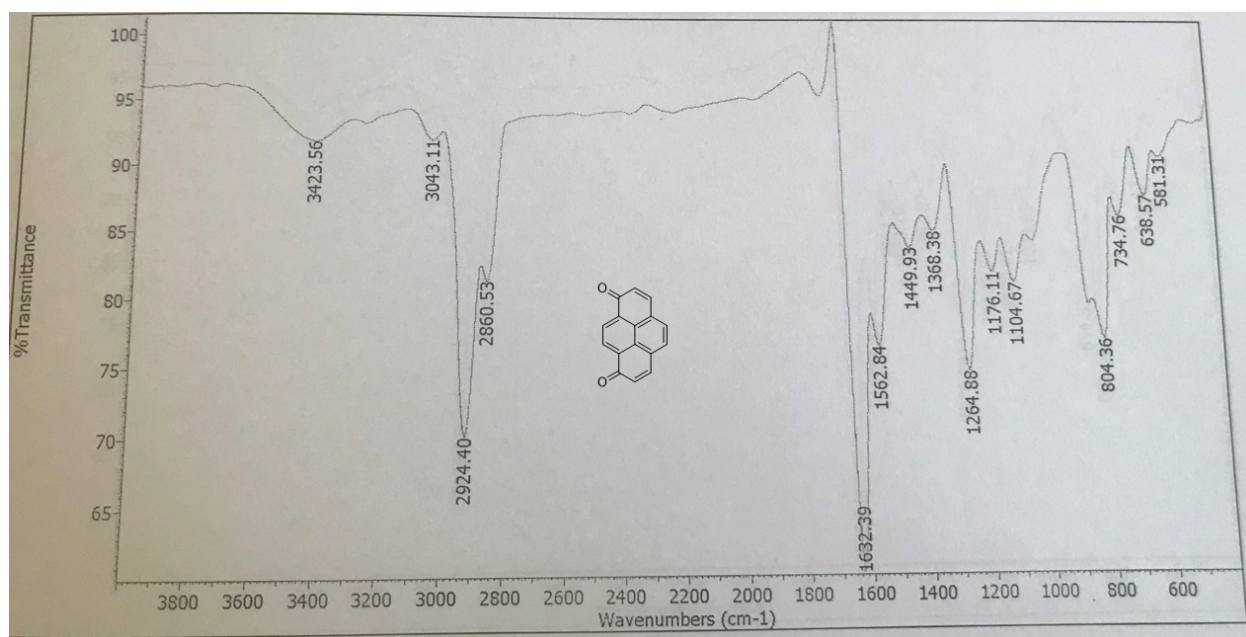


Fig. S53. FT-IR (KBr) of 6a.

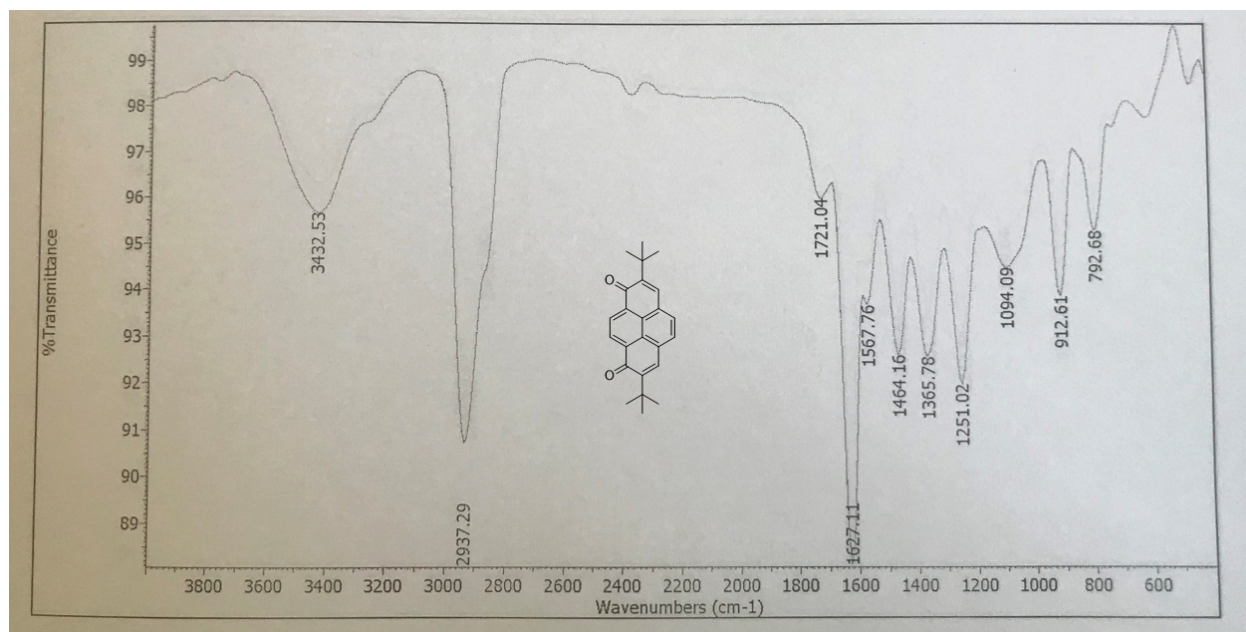


Fig. S54. FT-IR (KBr) of 6b.

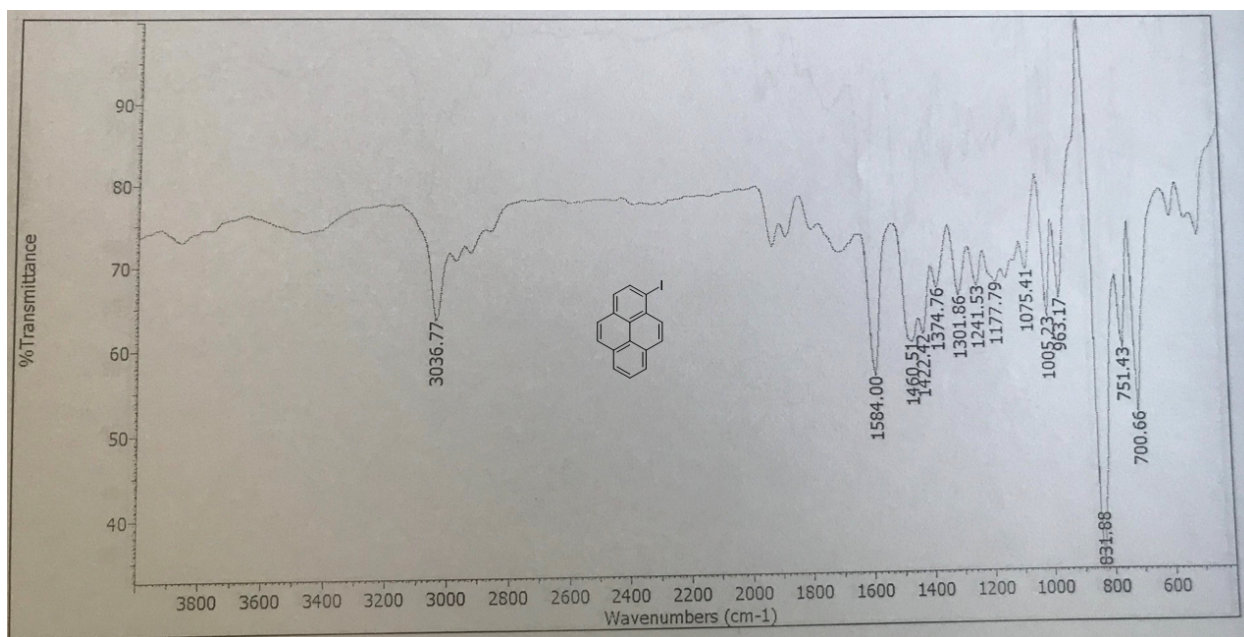


Fig. S55. FT-IR (KBr) of 7.

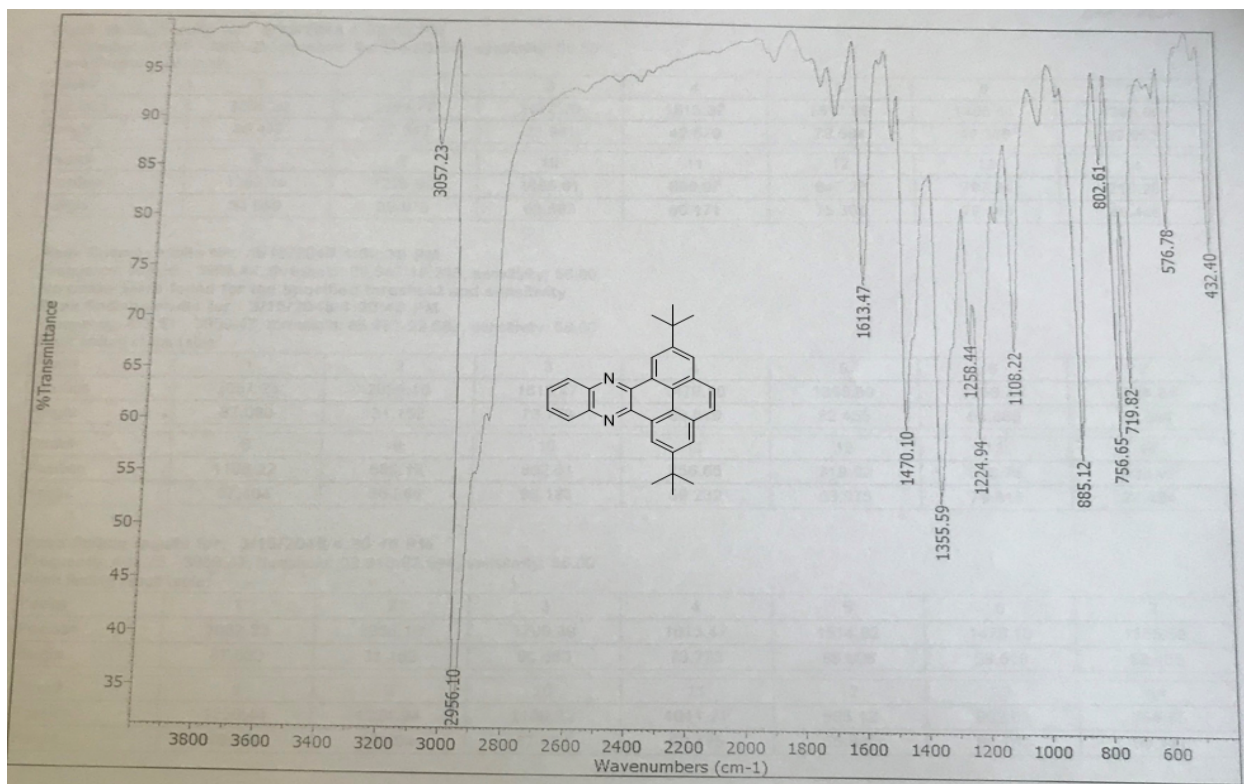


Fig. S56. FT-IR (KBr) of 8.

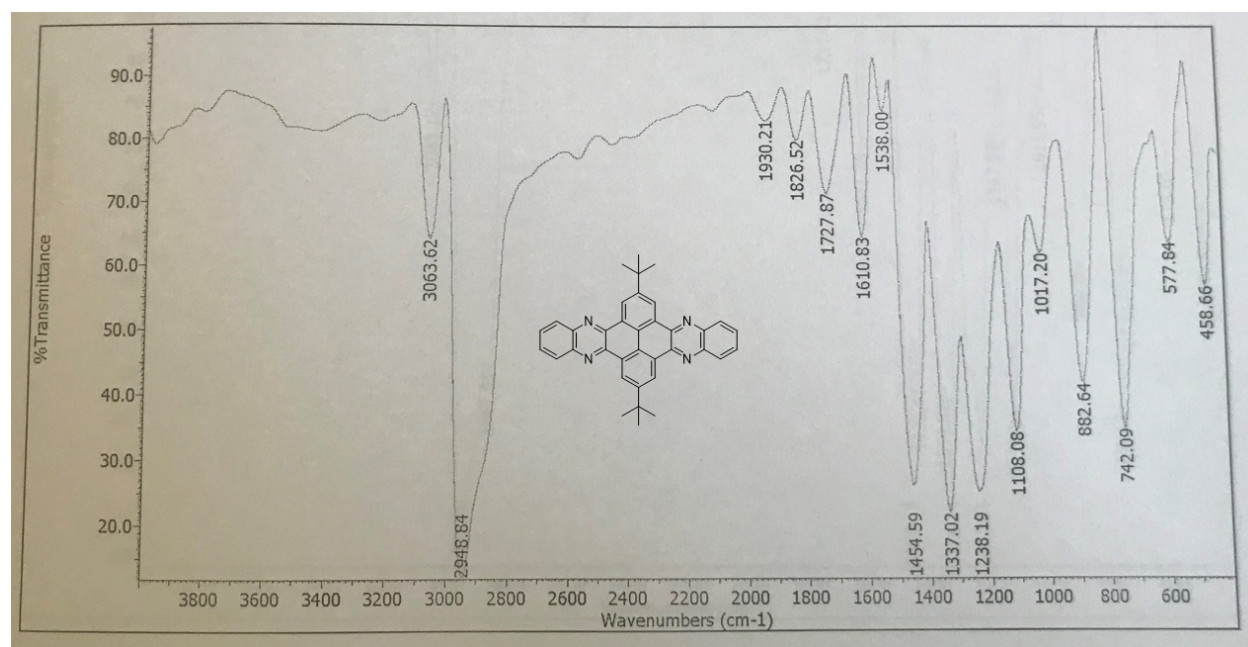


Fig. S57. FT-IR (KBr) of 9.

IX. References:

1. D. Prat, A. Wells, J. Hayler, H. Sneddon, C. R. McElroy, S. Abou-Shehada and P. J. Dunn, *Green Chem.*, 2016, **18**, 288-296.
2. J. Hu, D. Zhang and F. W. Harris, *J. Org. Chem.*, 2005, **70**, 707-708.
3. J. C. Walsh, K.-L. M. Williams, D. Lungerich and G. J. Bodwell, *Eur. J. Org. Chem.*, 2016, **2016**, 5933-5936.
4. D. Franz, S. J. Robbins, R. T. Boéré and P. W. Dibble, *J. Org. Chem.*, 2009, **74**, 7544-7547.
5. L. Rodenburg, R. Brandsma, C. Tintel, J. van Thuijl, J. Lugtenburg and J. Cornelisse, *Recl. Trav. Chim. Pays-Bas*, 1986, **105**, 156-161.
6. M. Frigerio, M. Santagostino and S. Sputore, *J. Org. Chem.*, 1999, **64**, 4537-4538.
7. A. G. Fallis and P. E. Tessier (2003). 2-Iodoxybenzoic acid (IBX). *E-EROS Encyclopedia of Reagents for Organic Synthesis*.
8. T. Stark, M. Suhartono, M. W. Göbel and M. Lautens, *Synlett*, 2013, **24**, 2730-2734.
9. H. Cho and R. G. Harvey, *J. Chem. Soc. Perkin Trans.*, 1976, 836-839.
10. Y. Zhang, X. Yang, H. Tang, D. Liang, J. Wu and D. Huang, *Green Chem.*, 2020, **22**, 22-27.
11. K. N. Parida and J. N. Moorthy, *J. Org. Chem.*, 2015, **80**, 8354-8360.
12. A. Khorshidi, *Chinese J. Catal.*, 2016, **37**, 153-158.
13. Y. Yamauchi, M. Yoshizawa, M. Akita and M. Fujita, *J. Am. Chem. Soc.*, 2010, **132**, 960-966.
14. T. Yamato, M. Fujimoto, A. Miyazawa and K. Matsuo, *J. Chem. Soc. Perkin Trans.*, 1997, 1201-1208.
15. P. K. Sahoo, C. Giri, T. S. Haldar, R. Puttreddy, K. Rissanen and P. Mal, *Eur. J. Org. Chem.*, 2016, **2016**, 1283-1291.
16. P.-L. Wang, S.-Y. Ding, Z.-C. Zhang, Z.-P. Wang and W. Wang, *J. Am. Chem. Soc.*, 2019, **141**, 18004-18008.
17. K. Van Aken, L. Strekowski and L. Patiny, *Beilstein J. Org. Chem.*, 2006, **2**, 3.
18. D. J. C. Constable, A. D. Curzons and V. L. Cunningham, *Green Chem.*, 2002, **4**, 521-527.